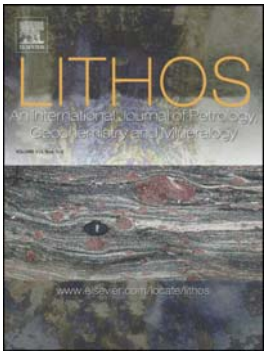

Melt extraction and enrichment processes in the New Caledonia lherzolites: Evidence from geochemical and Sr-Nd isotope data

Arianna Secchiari, Alessandra Montanini, Delphine Bosch, Patrizia Macera, Dominique Cluzel

PII: S0024-4937(16)30065-2
DOI: doi: 10.1016/j.lithos.2016.04.030
Reference: LITHOS 3916

To appear in: *LITHOS*

Received date: 1 December 2015
Accepted date: 29 April 2016

Please cite this article as: Secchiari, Arianna, Montanini, Alessandra, Bosch, Delphine, Macera, Patrizia, Cluzel, Dominique, Melt extraction and enrichment processes in the New Caledonia lherzolites: Evidence from geochemical and Sr-Nd isotope data, *LITHOS* (2016), doi: 10.1016/j.lithos.2016.04.030

Melt extraction and enrichment processes in the New Caledonia lherzolites: evidence from geochemical and Sr-Nd isotope data

Arianna Secchiari [1,2], Alessandra Montanini[1] , Delphine Bosch[2], Patrizia Macera[3], Dominique Cluzel[4]

[1] *Department of Physics and Earth Sciences, University of Parma , Parco Area delle Scienze 157/a, 43124 Parma; e-mail: arianna.secchiari@nemo.unipr.it*

[2] *Géosciences Montpellier, Université de Montpellier, Place Eugène Bataillon, 34095 Montpellier*

[3] *Earth Science Department, Pisa University, Via S Maria 53, 56126 Pisa*

[4] *Université de la Nouvelle Caledonie, Campus Nouville, 98851 Noumea*

Abstract

The New Caledonia ophiolite ("Peridotite nappe") is dominated by mantle lithologies, composed of forearc-related refractory harzburgites and minor lherzolites in both the spinel and plagioclase facies.

In this study, a comprehensive geochemical data set (major, trace elements and Sr-Nd isotopes) is used to constrain the mantle evolution of the lherzolites and their relationships with the basalts from the Poya terrane, which tectonically underlies the mantle rocks. The majority of the lherzolites are low-strain porphyroclastic tectonites. They likely record an asthenospheric origin followed by re-equilibration at lithospheric conditions, as supported by geothermometric estimates (T = 1100-940°C and 920-890°C for porphyroclastic and neoblastic spinel-facies assemblages, respectively). Olivine composition (Fo= 88.5-90.0 mol.%), spinel Cr# ([molar 100 • Cr/(Cr+Al)]= 13-17) and relatively high amounts (7-8 vol.%) of Al_2O_3- and Na_2O-rich clinopyroxene (up to 0.5 and 6.5 wt.%, respectively) indicate a moderately depleted geochemical signature for the spinel lherzolites. Bulk rock and clinopyroxene rare earth elements (REE) patterns display a typical abyssal-type signature, i.e. steeply plunging LREE accompanied by nearly flat HREE to

MREE. Clinopyroxene REE compositions of the spinel lherzolites may be reproduced by small amounts of fractional melting of a garnet lherzolite precursor (~4%), followed by 4-5 % melting in the spinel peridotite field. The plagioclase lherzolites show melt impregnation microstructures, Cr- and Ti-rich spinels and incompatible trace element enrichments (REE, Ti, Y, Zr) in bulk rocks and clinopyroxenes. Impregnation modelling for these elements suggests that the plagioclase lherzolites originated from residual spinel lherzolites by entrapment of highly depleted (non-aggregated) MORB melt fractions in the shallow oceanic lithosphere. Nd isotope compositions of the investigated peridotites are consistent with derivation from an asthenospheric mantle source that experienced a recent MORB-producing depletion event. This evolution was most likely accomplished in a spreading ridge. However, geochemical trace element modelling and Nd isotopes do not support a genetic mantle-crust link between the lherzolites and Enriched-MOR-type basalts from the Poya Terrane.

1.Introduction

Ophiolites have attracted much scientific interest since their recognition as surface exposures of fossil oceanic lithosphere accreted to continental margins (Dilek and Furnes, 2011 and references therein). The accessibility of ophiolitic sequences makes them an excellent natural laboratory for the study of oceanic lithosphere. Hence, field-based geochemical investigation of ophiolitic peridotites may prove valuable in understanding melt extraction and melt/rock interaction processes in the upper mantle. The genesis of oceanic lithosphere differs with geodynamic setting, i.e. mid-ocean ridge (MOR), ocean- continent-transition (OCT) and supra-subduction zone (SSZ) have distinct structural and chemical properties that permit their identification (Miyashiro, 1973; Pearce et al., 1984; Dilek and Furnes, 2011). Coexistence of peridotites with contrasting geochemical signatures indicative of MOR-type and SSZ-type melting regimes has been documented in other ophiolitic sequences (e.g. Lycian and Antalya ophiolitic complexes from Turkey, Aldanmaz et al., 2009, and Coast Range

ophiolites, Choi et al., 2008). Geochemical and mineralogical characteristics of mantle residua may be an effective tool to identify the geodynamic setting of ophiolite formation.

The New Caledonia Peridotite Nappe is one of the largest ophiolite complexes in the world. The ophiolite is dominated by mantle lithologies (mainly refractory harzburgites, together with minor lherzolites), locally capped by mafic-ultramafic cumulates. Although the New Caledonia mantle bodies have been the subject of several petrological and geochemical investigations starting from the 1980s (Prinzhofer et al., 1980; Dupuy et al., 1981; Nicolas and Dupuy, 1984; Prinzhofer and Allègre, 1985), the ultra-depleted nature of these rocks hampered their geochemical characterisation. In particular, isotopic data for the peridotites are still lacking, save for some Pb isotope data (Hamelin et al., 1984). Over the past decade, several petrological and geochemical investigations were undertaken, with a view to understanding the origin of the harzburgites and associated intrusive rocks (Marchesi et al., 2009; Ulrich et al., 2010; Pirard et al., 2013). These studies converged on the consensus that the harzburgites are of a SSZ affinity. In contrast, a relatively limited geochemical dataset is available for the lherzolites (Ulrich et al., 2010) meaning that their evolution and geodynamic affinity are poorly understood. Another debated issue concerns the existence of a genetic link between the New Caledonia lherzolites and the basaltic unit of Poya that tectonically underlies the Peridotite Nappe (Eissen et al., 1998; Marchesi et al., 2009; Whattam et al., 2009).

In order to bridge these gaps in knowledge, a comprehensive petrographic and geochemical characterisation of the main lherzolite bodies from New Caledonia are presented, in which we investigate melt extraction and melt-peridotite interaction processes. To this end, major and trace elements were determined in minerals and bulk rocks for selected samples of spinel and plagioclase lherzolites. In addition, Sr-Nd isotope data were obtained on bulk rocks and clinopyroxene separates to fingerprint the geochemical signatures of the New Caledonia lherzolites in the context of mantle endmembers. Finally, we

evaluate the relationship between the lherzolites and the oceanic basalts from the Poya terrane.

2. Geological and petrological background

New Caledonia is located in the South West Pacific ocean. The island represents the northern extension of the Norfolk Ridge (Fig. 1) and is composed of a complex association of volcanic, sedimentary and metamorphic terranes ranging in age from Permian to Miocene (Aitchison et al., 1995a; Cluzel et al., 1994, 2001, 2012; Lagabrielle et al., 2013). In particular, New Caledonia can be subdivided into four main geological domains (Cluzel et al., 2001): (i) the Basement units (pre-Late Cretaceous basement and Late Coniacian-to-Late Eocene sedimentary cover), (ii) the Cenozoic high-pressure metamorphic belt, (iii) the basaltic Poya Terrane and (iv) a large slab of obducted peridotites, the Peridotite Nappe.

The Peridotite nappe is an allochtonous sheet of oceanic lithosphere from the Loyalty Basin (Fig. 1) thrust from NNE to SSW over the continental basement of the island in the Late Eocene (Prinzhofer et al., 1980; Collot et al., 1987). Its emplacement has been related to the failed subduction of the New Caledonia continental basement in a NE-dipping subduction zone, which culminated with the obduction of the Loyalty oceanic lithosphere (Cluzel et al., 1998). The Peridotite Nappe overlies the basaltic Poya Terrane, separated by a sub-horizontal thrust fault and a thick (50-200 m) sole of serpentinite mylonites, locally associated with high-temperature amphibolite lenses formed during subduction initiation in the Early Eocene (Cluzel et al., 2012).

The Peridotite nappe is largely exposed in the Massif du Sud (Fig. 1), a thick harzburgite-dunite sequence with kilometre-scale lenses of mafic and ultramafic cumulates at the top (Pirard et al., 2013). The cumulates crystallised from ultra-depleted melts, most likely in a nascent arc environment (Marchesi et al., 2009; Pirard et al., 2013). Large klippen of peridotites also occur along the west coast (Fig. 1), in the Isle of Pines (south) and Belep Islands (north). Smaller klippen are exposed in the central chain, and a few

kilometre-scale lenses of peridotite are included in the HP-LT metamorphic complex.

The New Caledonia harzburgites are highly depleted peridotites, as evidenced by the absence of primary clinopyroxene and exceedingly low whole-rock trace element contents (Prinzhofer and Allegre, 1985). Recent geochemical studies (Marchesi et al., 2009; Ulrich et al., 2010) invoke a complex history in the formation of these rocks, in which melting, melt-rock interaction and re-melting, gave rise to their ultra-depleted compositions.

Lherzolitic rocks occur only in the northern part of New Caledonia, where they form discrete ultramafic bodies (Poum and Tiébaghi Massifs, Fig. 1). These bodies are mostly composed of spinel and plagioclase lherzolites, with minor cpx-bearing harzburgites and dunite-harzburgites (Sécher, 1981; Nicolas and Dupuy, 1984; Leblanc, 1995). Centimetre-thick pyroxenite dikes may be common, especially in the plagioclase lherzolites from the Poum massif (Nicolas and Dupuy, 1984; Leblanc, 1995).

In the lherzolites, the widespread development of superimposed structures testifying evolution from high-temperature ductile to fragile deformation, has been related to the presence of a major shear zone that runs along the northeastern side of Belep Islands and Poum and Tiebaghi massifs. This high-strain zone, characterised by a steeply dipping foliation, has been interpreted as a palaeo-transform fault (Secher, 1981; Nicolas, 1989) that was reactivated at shallower conditions during and after obduction (Titus et al, 2011). In the Poum massif, plagioclase lherzolites with mylonitic to protomylonitic textures grade into relatively undeformed plagioclase and spinel lherzolites and, finally, cede to harzburgites, moving away from the shear zone (Secher, 1981). Acccording to Leblanc (1995), the harzburgites represent more depleted asthenospheric material channeled along the transform fault.

The Poya terrane is mainly composed of massive and pillow basalts intruded by rare dolerite dikes. Tholeiitic basalts with Enriched-MORB affinity predominate, and are associated with minor occurrences of back-arc basin basalts (BABB) and ocean island basalts (OIB) (Cluzel et al, 1997; Eissen et al., 1998; Cluzel et al., 2001). These variable geochemical signatures suggest derivation from a

variety of mantle sources. The Poya basalts are tectonically interlayered with thin (1-3 m) radiolarian-bearing pelagic sediments, which constrain the timing of basalt eruption between Campanian and Late Paleocene-Early Eocene (Aitchison et al, 1995b; Cluzel et al., 2001).

3. Sampling and petrography

Due to widespread serpentinisation, fresh peridotite exposures are rare. After extensive exploration and careful sampling, nine samples from the Babouillat (Tiebaghi massif) and Poum outcrops (Fig.1) were chosen for this study, together with two basaltic lavas from the Poya terrane.

In the peridotites, olivine is partially replaced by serpentine+magnetite assemblages exhibiting mesh structures, whereas ortho- and clinopyroxenes are not affected by serpentinisation. Other secondary minerals are represented by small amounts of chlorite, talc and tremolitic amphibole as rare overgrowths on pyroxenes. Spinel lherzolites are clinopyroxene-poor (up to 7-8 vol.%), medium- to fine-grained rocks, characterised by a porphyroclastic texture (Fig. S1a) with local protomylonite development.

Olivine occurs as kinked and elongated porphyroclasts, forming the main foliation. Orthopyroxene porphyroclasts are coarse-grained crystals (sometimes up to 5-6 mm across) with a rounded habit. They also occur as elongate grains parallel to the foliation, and show evidence of ductile deformation (undulose extinction and kink bands) and exsolution lamellae of clinopyroxene. Large orthopyroxenes frequently display embayments filled by undeformed olivine crystals (Fig. S1a). Small, undeformed and exsolution-free orthopyroxene grains are found in association with recrystallised olivine, spinel and clinopyroxene. Exsolved clinopyroxene porphyroclasts occur as smaller (up to 1-2 mm), light green-brownish crystals in apparent equilibrium with the primary assemblage (Fig. S1b). Yellow-brown spinels display irregular or rounded shapes. Holly-leaf shaped grains are sometimes found between olivine and pyroxene porphyroclasts.

Plagioclase lherzolites are characterised by medium- to coarse-grained porphyroclastic textures. Plagioclase occurs as interstitial blebs, irregular patches or rims around spinel (Fig. S1c) and are often sericitised. Clinopyroxene porphyroclasts show very irregular shapes, frequent embayments and partial replacement by orthopyroxene + plagioclase aggregates. Olivine may be rimmed by secondary orthopyroxene.

4.Analytical techniques

Major element mineral analyses were performed at the Physics and Earth Sciences Department in Parma using a JEOL-6400 electron microprobe equipped with a LINK-ISIS energy dispersive microanalytical system. The electron beam was produced at an accelerating voltage of 15 kV and probe current of 0.25 nA; and both natural minerals and synthetic compounds were used as standards.

The samples for bulk rock analyses were sawn into thin slabs and altered parts were carefully removed before crushing. In order to obtain representative major and trace element analyses, rock powders were prepared from at least 1 kg of material and crushed to powders in an agate mill.

Whole-rock major-element oxides and Ni, Co, Cr, V, Zn were measured by conventional XRF techniques at the Department of Chemical and Geological Sciences in Modena using a wavelength dispersive X-ray fluorescence spectrometer (Philips PW 1480).

Whole-rock and in situ trace element analyses were performed at the AETE technical platform ("Trace Element Analysis in the Environment", Université de Montpellier). Bulk trace element concentrations (excluding Ni, Co, Cr, V, Zn) were determined using a ThermoFinnigan ELEMENT XR (HR-ICP-MS: high resolution inductively coupled plasma mass spectrometer) after acid digestion with HNO_3-HF-$HClO_4$, as described by Ionov et al. (1992). Replicate analyses of international standards and three investigated samples (BA1, BAB2A, POU2B) are reported in Table S1.

Trace element compositions of clinopyroxenes were measured in-situ on polished thick sections (thickness = 120 µm) by ThermoFinnigan ELEMENT XR high resolution (HR) ICP-MS coupled with a Geolas Lambda Physik CompEx 102 excimer. Signals were acquired in Time Resolved Acquisition, wherein the background was measured for 2 minutes compared with 1 minute for the sample. The laser was fired at an energy density of 15 J/cm^2 and a frequency of 8-10 Hz, using a spot size of 102 µm. Si was used as internal standard and analyte concentrations were calibrated against the NIST 612 rhyolitic glass, according to the values of Pearce et al. (1997). Data were subsequently reduced using the GLITTER software by inspecting the time-resolved analysis and selecting time intervals in which signal intensities were homogeneous. Our data for the international standard reference material BIR-1G shows good agreement with published values.

For isotope analyses, powdered samples were weighed to obtain approximately 100-200 ng of Sr and Nd. A 1 hour 6 N HCl leaching step at 95 °C was performed before acid digestion. After leaching, residues were rinsed three times in Milli-Q H_2O. The samples were subsequently dissolved during 72 h on a hot plate with a mixture of HF and HNO_3. After evaporation to dryness, 2 ml of HNO_3 was added to the residue and kept at 95°C for 24–48 h.

Strontium isotopes were separated using Sr Eichrom resin (Pin et al., 1994), while Neodymium isotopes were separated in two steps, a first using AG50W-X12 cation exchange resin followed by a second to purify REE using HDEHP conditioned Teflon columns.

Sr isotopic ratios were measured by thermal ionization mass spectrometry using a Triton Finnigan Mat spectrometer from the Labogis from the Nîmes University. $^{87}Sr/^{86}Sr$ isotopic ratios were normalised using a value of 0.1194 for the $^{86}Sr/^{88}Sr$ ratio. The NBS987 standard, analysed during the course of this study, yielded an average $^{87}Sr/^{86}Sr$ of 0.710245.

$^{143}Nd/^{144}Nd$ isotopic composition was determined by multi-collector inductively coupled plasma mass spectrometry (Finningan Neptune Plus) at the Ecole Normale Supérieure de Lyon (ENSL). Average values were 0.511971 ± 10 (2σ) (n = 10) for the AMES-Rennes (Chauvel and Blichert-Toft, 2001) Nd standard.

5.Major element mineral chemistry

The forsterite content of olivine in the spinel and plagioclase lherzolites is rather homogenous (88.5-90.0 mol.%).

Representative major element mineral compositions of clino- and orthopyroxenes are reported in Table S2. Orthopyroxene is enstatitic with an average composition $Wo_{0.01-0.03}$ $En_{0.84-1.02}$ $Fs_{0.11-0.14}$. and Mg# [$(Mg/(Mg+Fe^{2+})$] between 0.88-0.90. Orthopyroxene mirrors the behaviour of olivine, with no significant compositional difference between spinel and plagioclase lherzolites in terms of Mg#. TiO_2 contents are generally very low (< 0.10 wt.%). The cores of orthopyroxene porphyroclasts in the spinel lherzolites are Al_2O_3-rich (4.9-5.9 wt. %) and have Cr_2O_3 contents varying between 0.63-0.90 wt.%. Al_2O_3 and Cr_2O_3 slightly decrease from core to rim, whereas distinctly lower values are observed in neoblastic orthopyroxenes (Al_2O_3 = 2.4-3.2 wt. % and Cr_2O_3 = 0.57-0.19 wt.%, respectively), most likely as a result of synkinematic spinel crystallisation. As a whole, porhyroclastic and neoblastic orthopyroxenes from plagioclase lherzolites show decreasing Al_2O_3 contents between porphyroclast cores and neoblasts (5.6-3.2 wt.% and 2.3-1.8 wt.%, respectively), whereas no substantial Cr_2O_3 variation is observed. The orthopyroxene crystals in plagioclase-orthopyroxene aggregates have low Al_2O_3 (1.8-2.3 wt.%) and Cr_2O_3 concentrations ranging between 0.44-0.90 wt.%, in agreement with the concomitant crystallisation of plagioclase.

Clinopyroxene is diopsidic with relatively high Na_2O and Al_2O_3 contents and Mg# varying between 0.90-0.92. Porphyroclastic clinopyroxene cores from spinel and plagioclase lherzolites have similar Al_2O_3 contents (5.3-6.7 and 5.0-6.4 wt.%, respectively). Spinel-facies clinopyroxene porphyroclasts have slightly higher Na_2O contents (0.48-0.58 wt.%) and lower Cr_2O_3 (0.80-1.0 wt.%) than those from plagioclase lherzolites (Na_2O = 0.25-0.40 wt. % and Cr_2O_3 = 1.2-1.4 wt.%). A moderate decrease of Al_2O_3 and Na_2O is observed in porphyroclast rims and in the neoblastic clinopyroxene of spinel lherzolites.

Spinel compositions (Table S3) show significant differences between spinel and plagioclase lherzolites. In spinel lherzolites, Cr# and Mg# vary between 0.132-0.167 and 0.732-0.759, respectively. Plagioclase-bearing lherzolites are characterised by considerably higher Cr# (0.484-0.624) and lower Mg# (0.375-0.551). High Cr# of spinel from plagioclase lherzolites is associated with elevated TiO_2 (0.2-0.5 wt.%), whereas TiO_2 is generally < 0.15 wt.% in spinel lherzolites (Fig. 2c).

Mg#-Cr# relationships for spinel are shown in Fig. 2a. Spinel compositions of the New Caledonia harzburgites have been also reported for comparison. Spinels from spinel lherzolites display compositions similar to those of abyssal (i.e. mid-ocean ridge) peridotites. In contrast, spinels from plagioclase lherzolites are characterised by lower Mg# and higher Cr#, similar to the refractory harzburgites.

Compositional relationships between olivine and chromian spinel are illustrated in Fig. 2b. The compositions of spinel from the spinel lherzolites fall in the range of passive margin lherzolites, very close to the field of abyssal peridotites. In contrast, Mg# and Cr# composition for plagioclase lherzolites plot off the mantle array.

Ca-rich plagioclase (anorthite ~ 88 mol. %) has been analysed in one sample (POU1A) where tiny relict patches of fresh plagioclase have been preserved.

6. Geothermometry

Equilibrium temperatures for the lherzolites were calculated on the basis of mineral composition data obtained by microprobe analyses.

Ca-Mg exchange between Cpx-Opx and Ca-in-orthopyroxene geothermometers of Wells (1977) and Brey and Kohler (1990) were applied to estimate the equilibrium temperatures of both porphyroclastic and neoblastic assemblages of spinel lherzolites, for an assumed confining pressure of 1.5 GPa. To avoid the uncertainties related to Fe^{3+} recalculations, all iron in pyroxenes was assumed to be Fe^{2+}. This assumption has negligible effects on two-pyroxene thermometry, as discussed by Canil and O' Neill (1996).

The cores of spinel-facies orthopyroxene porphyroclasts yield $T_{(Ca\text{-}in\ Opx)}$ between 1030-1095°C, whereas two-pyroxene porphyroclast temperatures vary over a wider range (940-1080°C). The lower T values obtained using two-pyroxene geothermometry are related to pyroxene exsolution during cooling. Preservation of Ca-rich domains in orthopyroxene, on the other hand, is a consequence of low diffusivity of Ca in orthopyroxene compared to high Ca-Mg diffusivity in clinopyroxene (Lenoir et al., 2001; Montanini et al., 2006). Core-to rim compositional variations in the orthopyroxene porphyroclasts locally reflect cooling of ca. 50-100°C. Temperatures obtained with pyroxene thermometry for neoblastic assemblage of spinel lherzolites are shifted towards lower values (890-920°C).

We have also applied the Ca-in-orthopyroxene geothermometer to the plagioclase lherzolites for an assumed pressure of 0.8 GPa. The slightly higher T obtained for porphyroclastic (980-1120°C) and neoblastic assemblages (960-1070°C) are possibly related to the melt impregnation process (see section 8.2).

Pressure is difficult to constrain owing to the lack of appropriate geobarometers in garnet-absent systems. The pressure of the garnet–spinel transition in peridotitic systems is mainly controlled by the Cr content of the spinel (O'Neill, 1981; Webb and Wood, 1986; Klemme, 2004). In particular, spinel is stabilised to higher pressures with increasing Cr/(Cr+Al). A maximum pressure estimate for the spinel facies can be determined by the formulation of Webb and Wood (1986). Using the composition of spinel porphyroclast cores not rimmed by plagioclase, the obtained maximum pressure is 2.2 GPa.

7.Geochemistry

7.1. Major and trace element bulk rock composition

Whole-rock major- and trace element contents of lherzolites are reported in Table 1. LOI values, ranging between 6.39 and 10.69 wt.%, reflect moderate degrees of serpentinisation. Nevertheless, projection of the data onto a MgO/SiO_2-Al_2O_3/SiO_2 diagram (Fig. S2) shows that the analysed peridotites

plot close to the terrestrial array defined by fresh mantle rocks. This indicates that their major element composition was not affected by significant chemical exchange related to seafloor alteration.

Plagioclase and spinel lherzolites show similar major element compositions, except for their Al_2O_3 and CaO contents, which are shifted to higher values in plagioclase lherzolites (Table 1, Fig. 3). Al_2O_3 and CaO vary between 1.30-2.83 wt.% and 1.26-2.20 wt.% respectively. Both lherzolite types display variable degrees of depletion, with MgO ranging from 36.7 to 40.8 wt.%. Negative correlations of Al_2O_3, SiO_2 and CaO vs. MgO are observed (Fig. 3).

Chondrite-normalised REE patterns are plotted in Fig. 4a. The analysed samples are characterised by higher MREE-HREE abundances than the LREE, where Nd_N/Sm_N = 0.19-0.27 and Nd_N/Yb_N = 0.03-0.07 for Yb_N = 0.99-1.30. They broadly exhibit positively-sloping patters, where HREEs are more abundant than MREEs (Tb_N/Yb_N = 0.59-0.70). On the whole, these patterns closely resemble those of modern abyssal peridotites (e.g. Pearce et al., 2000).

Spinel and plagioclase lherzolites have REE patterns that are subparallel to one another, though the plagioclase-bearing varieties are typified by higher MREE-HREE contents. A slight enrichment in La-Ce, particularly in the spinel lherzolites, is also observed (Fig. 4a).

Extended multi-element diagrams normalised to Primitive Mantle (PM) are reported in Fig. 4b. Patterns are subparallel for spinel and plagioclase lherzolites from Ce. Cs is enriched only in plagioclase lherzolites, especially in the samples from Babouillat (BAB1B and BAB2B). Rb and Ba are commonly enriched with respect to adjacent elements. Positive Pb and Sr anomalies are present in all samples, as are pronounced negative Zr anomalies.

Whole rock compositions and chondrite-normalised REE patterns of two Poya basalts are reported in Table 1 and Fig. S3. The basalts display nearly flat REE patterns, with abundances between 15-20 times chondritic values.

7.2. Clinopyroxene trace element composition

Trace element concentrations and chondrite-normalised REE patterns for the analysed clinopyroxenes are reported in Table S4 and Fig. 5.

Clinopyroxene from spinel and plagioclase lherzolites have subparallel patterns. Slightly higher REE contents are observed in the plagioclase-bearing rocks (Fig. 5a). Clinopyroxenes have strongly depleted LREE abundances but relatively flat HREE (Tb_N/Yb_N= 0.72-1.01) and MREE/HREE fractionation (Sm_N/Yb_N = 0.27-0.50). The lherzolite patterns closely resemble those of clinopyroxenes from abyssal peridotites (Johnson et al., 1990; Hellebrand et al., 2002; Brunelli et al., 2006; Warren et al., 2009). Clinopyroxenes from spinel lherzolites are also characterised by a small La-Ce enrichment. Small negative Eu anomalies (Eu/Eu* = 0.77-0.92), occur in the clinopyroxenes from plagioclase lherzolites, as a result of equilibration with plagioclase.

The absolute concentrations of the most incompatible trace elements (from Cs to Pb) are generally higher in the clinopyroxene from the plagioclase lherzolites (Fig. 5b). Negative anomalies for Ba and Pb enrichment are observed. Clinopyroxene from spinel and plagioclase lherzolites display similar and convex upward patterns from Sr to Lu, with higher absolute concentrations for plagioclase lherzolites. Sr invariably shows negative anomalies, as well as Zr, which is decoupled from the neighbouring Hf.

7.3. Sr-Nd isotope composition

Sr and Nd isotopic ratios are reported in Table 2. $^{87}Sr/^{86}Sr$ and $^{143}Nd/^{144}Nd$ have been determined for six lherzolites, one clinopyroxene fraction from the lherzolite sample BA1 and two basaltic lavas from the Poya Unit. All the samples have been corrected for radiogenic ingrowth assuming an age of 53 Ma, i.e. the inferred timing of subduction inception (Cluzel et al., 2006).

Lherzolites display initial $^{143}Nd/^{144}Nd$ ratios between 0.512930-0.513134 and $^{87}Sr/^{86}Sr$ between 0.705782-0.707527. The corresponding values of $\varepsilon_{Nd(i)}$ vary from +6.98 to +10.97, while $\varepsilon_{Sr(i)}$ is more variable, ranging from +19.19 to +43.85. A slight difference can be detected for $^{87}Sr/^{86}Sr$ values between Babouillat and Poum localities, with more radiogenic values obtained for Poum ($\Delta^{87}Sr/^{86}Sr$ =0.00123).

The clinopyroxene separate from the spinel lherzolite BA1 yields initial values of 0.705791 for $^{87}Sr/^{86}Sr$ and 0.512982 for $^{143}Nd/^{144}Nd$, in good agreement with the initial value obtained for the bulk rock (0.706128 and 0.513005 for $^{87}Sr/^{86}Sr$ and $^{143}Nd/^{144}Nd$, respectively). Sr isotopic ratios of bulk rock and coexisting clinopyroxenes are significantly more radiogenic than DMM values, whereas Nd isotope compositions are more akin to a depleted asthenospheric mantle source (e.g. Hofmann, 2003).

In a Sr-Nd isotope diagram (Fig. 6) the lherzolite samples define a subhorizontal trend, falling outside the fields of both abyssal peridotites and Pacific arc volcanics, as a result of highly radiogenic Sr isotope compositions.

The two basalts from the Poya terrane have similar Sr and Nd initial isotopic ratios ($^{87}Sr/^{86}Sr$ = 0.70407 and 0.70442, $^{143}Nd/^{144}Nd$ = 0.51285 and 0.51284 for the samples KO1 and BOU1, respectively). They plot in the Pacific arc domain and fall close to the compositions of Poya basalts with E-MORB affinity (Cluzel et al., 2001). As a whole, the Poya basalts are distinguished from the lherzolites by less radiogenic Sr and Nd isotopic compositions.

8. Discussion

8.1. Evaluation of partial melting processes: garnet involvement ?

The New Caledonia lherzolites have a depleted chemical signature and show remarkable similarity to abyssal peridotites. To assess whether major element variation in the lherzolites is brought about by partial melting, trends are compared with the anhydrous melting curves calculated by Niu (1997). Fractional melting curves in the interval 2.5-0.8 GPa (fractional melting degree ≤ 0.25) and 1.5-0.8 GPa (fractional melting degree ≤ 0.15) are shown in Fig. 3. Isobaric batch melting curves for 1 and 2 GPa are also plotted for comparison. The spinel lherzolite samples fall on the polybaric fractional melting curves between 2.5-0.8 GPa in the Al_2O_3-MgO and CaO-MgO plots, and plot close to the curves in the SiO_2–MgO and FeO_{tot}–MgO diagrams. Their major element compositions are therefore consistent with partial melting

residues. On the other hand, the plagioclase lherzolites depart from the melting curves, being characterised by higher Al_2O_3 contents and lower CaO and SiO_2 concentrations. Hence, the compositions of the plagioclase lherzolites are not compatible with products of partial melting, rather they reflect additional processes that will be discussed in section 8.2.

The observed major element trends discussed above suggest that the widespread occurrence of orthopyroxene embayments filled by olivine in spinel lherzolites may be ascribed to incongruent melting of orthopyroxene, characteristic of decompression melting beneath oceanic ridges (Niu, 1997). These textures could be also related to reactive porous flow of pyroxene-undersaturated melts (e.g. Piccardo et al., 2007; Rampone et al., 2008). Neverthless, the absence of chemical evidence, such as the decrease of SiO_2 and increase of FeO^T against MgO, resulting from olivine addition during melt migration, argues against this interpretation.

A rough estimate of the degree of partial melting for the spinel lherzolites can be obtained adopting the method of Hellebrand et al. (2001), which is based on the Cr# value of spinel ($F = 10 \cdot (\ln Cr\#) + 24$). Applying this equation to the spinel porphyroclast cores of spinel lherzolites (Table S3), low degrees of partial melting were inferred (4-5% and 5-6% for the samples BA1 and POU2, respectively). This method, however, may underestimate the degree of bulk melting of the peridotites, as Cr# values can be strongly affected by subsequent refertilisation. To provide further constraints on the partial melting process, we carried out trace element modelling based on whole rock and clinopyroxene trace element compositions. We initially applied a non-modal fractional melting model, using the equations of Albarede (1996) and assuming that melting occurred entirely in the spinel stability field. Details of the model and adopted partition coefficients are reported in Table S5.

The results, shown in Fig. 7a, indicate that HREE patterns of spinel lherzolites are broadly consistent with low melting degrees (6-8%) of a depleted mantle source, whereas MREE would require higher degrees of melting. Similar discrepancies have been also observed applying fractional melting model to reproduce the clinopyroxene REE composition of spinel lherzolites (Fig. 7b). For

the clinopyroxene, estimated melting degrees vary between 4% and 7%. Moreover, La-Ce enrichments are not consistent with melting processes and they will be discussed later (see section 8.3).

On the whole, fractional melting under spinel facies conditions fails to reproduce the REE patterns of spinel lherzolites. In particular, relatively low MREE/HREE ratios are coupled with high Yb_N in clinopyroxene and whole rock. These features are characteristic of peridotites that experienced an initial stage of melting in the presence of residual garnet (Hellebrand et al., 2002; Müntener et al., 2004). Garnet involvement in mid-ocean ridge melting processes has been often invoked to explain geochemical features of MORB (e.g. Salters and Stracke, 1989; LaTourrette et al., 1993; Hischmann and Stolper, 1996) and abyssal and ophiolitic peridotites (Johnson et al., 1990; Hellebrand et al., 2002; Barth et al., 2003).

The relatively high Na_2O content of clinopyroxenes from spinel lherzolites (Table S2) compared with their very low Nd abundances (Nd_N = 0.24-0.33) are also consistent with a polybaric melting scenario. In fact, Na compatibility during partial melting increases with increasing pressure whereas Nd behaviour is nearly constant, as discussed by Müntener et al. (2010). The Na_2O and Nd contents of the Poum and Babouillat clinopyroxenes (samples POU2 and BA1, respectively) plot on polybaric melting curves calculated by Müntener et al. (2010), which include 4 % melting in the garnet field. Notably, melting of a spinel peridotite source would lead to a stronger Na depletion in the clinopyroxene. Major element covariation diagrams for the spinel lherzolites (Al_2O_3 and CaO vs. MgO, Fig. 3) are also consistent with melting starting at pressures around 2.5 GPa, i.e. close to the boundary between garnet- and spinel-stability field near the fertile peridotite solidus (Takahashi and Kushiro, 1983). On the basis of the estimated pressure for the garnet-spinel transition in the investigated lherzolites (~2.2 GPa, see section 6) the garnet melting stage may be tentatively constrained to the 2.5-2.2 GPa interval.

Hence, polybaric fractional melting of a depleted mantle source starting in the garnet stability field, followed by additional melting in the spinel field, was also computed for REE and other incompatible trace element data (Sr, Zr, Hf, Y,

Ti). The obtained patterns (Fig. 8) faithfully replicate the observed whole rock and clinopyroxene compositions. In particular, 4% of melting in the garnet stability field followed by 4-5% melting in the spinel stability field is required to reproduce the REE patterns of clinopyroxenes from the Poum (sample POU2), and Babouillat massif (sample BA1).

A good agreement is also found for the other trace element data, with the exception of Zr, which is invariably lower than the predicted values. Although the occurrence of Zr depletion in mantle clinopyroxenes has been documented by various authors (Salters and Shimizu 1988; Johnson et al. 1990; Rampone et al. 1991; McDonough et al. 1992), its origin remains uncertain. Negative Zr anomalies in clinopyroxene may be balanced by corresponding positive anomalies in orthopyroxene as a result of different partitioning behaviour between mantle minerals (Rampone et al., 1991; McDonough et al. 1992). However, this cannot produce the observed bulk rock Zr anomalies (Fig. 4-5). During spinel field partial melting, Zr and Hf do not behave coherently, i.e. Zr is more incompatible than Hf ($D_{bulk,\ Zr}/D_{bulk,\ Hf} \sim 0.5$, see also Table S5 and Niu, 2004), leading to strong Zr depletion in the residuum. In a garnet-bearing assemblage, however, the difference of compatibility is negliglible, significantly reducing the Zr anomaly (see Fig. 8). Alternatively, the occurrence of such prominent Zr/Hf fractionation in both residual whole rocks and clinopyroxenes could be the consequence of chromatographic effects related to melt percolation at low melt/rock ratios, as proposed by Niu (2004).

The onset of melting in the garnet stability field indicates that the melting region extended to great depths (possibly exceeding 70-80 km). This deepening of the melting column may be related to high potential mantle temperatures or the degree of mantle fertility (e.g. see Brunelli et al., 2006). On the other hand, the estimated bulk degree of melting does not exceed 8-10 %, and the melting in the spinel stability field is limited, which suggests that conductive cooling from above prevented protracted decompression melting to shallower levels. Such a melting regime is typical of slow-spreading ridges (e.g. Hellebrand et al., 2002) or may indicate proximity of the investigated peridotites to a transform fault (Nicolas, 1989; Leblanc, 1995).

8.2. Origin of the plagioclase lherzolites

In peridotitic rocks, plagioclase rims around spinel may form during subsolidus evolution from spinel-to plagioclase facies conditions or as a result of a reaction involving a melt. Metamorphic equilibria governing the spinel-to plagioclase-facies transition (enstatite + diopside + spinel = anorthite + forsterite and enstatite + Cat-Tsch = anorthite + forsterite, Rampone et al., 1993) imply formation of olivine together with plagioclase during subsolidus transformations. In contrast, we observe formation of a new generation of orthopyroxene together with plagioclase, at the expense of clinopyroxene and olivine. Textural evidence thus argues against a closed system subsolidus evolution from spinel- to plagioclase-facies conditions, suggesting that plagioclase crystallisation may be related to a reaction with (SiO_2-saturated) melt.

Spinel composition (Fig. 2) provides further support for this hypothesis. In fact, the plagioclase lherzolites contain spinels with significantly higher Cr# than spinel lherzolites, partially overlapping those of refractory harzburgites in New Caledonia, although at lower Mg#. Remarkably, these spinels plot outside the partial melting trend defined by the Cr#-Mg# mantle array. High and variable Cr# values are also associated with distinctly higher TiO_2 contents (0.21-0.49 wt.%) compared to spinel lherzolites (Fig. 2c). Similar compositional variations of spinel are commonly observed in plagioclase peridotites that were affected by melt/rock interaction processes (e.g. Dick and Bullen, 1984; Cannat et al., 1990; Seyler and Bonatti, 1997; Kaczmarek and Müntener, 2008).

The formation of plagioclase lherzolites is also accompanied by Al_2O_3 and CaO increase and incompatible trace element enrichment with respect to the spinel lherzolites (Fig. 3-5). The chemical modifications associated with plagioclase crystallisation may derive from simple melt entrapment and trace element re-equilibration of minerals with the melt (Müntener et al., 2010) or may be related to a process where the infiltrating melt reacts with the solid to variable extents (e.g. Rampone et al., 2008).

To provide further constraints on the impregnation process we have first attempted to simulate the chemical effect of simple melt entrapment in a spinel-bearing residual lherzolite. We have calculated the trace element composition (REE, Zr, Y, Ti) of clinopyroxene equilibrated with a plagioclase-bearing assemblage produced from mixing between a spinel lherzolite protholith and small fractions of different liquids with highly depleted compositions. The liquids used for the simulation were a "boninite"-like melt and an incremental melt fraction derived from a depleted asthenospheric mantle source under spinel-facies conditions. The resulting clinopyroxene compositions are reported in Fig. 9. For both types of liquid, the models fail to reproduce the convex-up REE patterns and distinctly higher MREE-Y contents in the observed clinopyroxenes. On the other hand, assuming higher proportions of trapped melt would overestimate the calculated bulk rock compositions. Models involving more enriched liquids, e.g. aggregated MORB melts generated by variable degrees of partial melting (5-15 %), are not applicable because they would produce impregnated rocks with significantly higher incompatible element enrichments (up to an order of magnitude), even for very small amounts of melt (1-2%).

Textural evidence (e.g. widespread occurrence of embayed clinopyroxene porphyroclasts and the local presence of orthopyroxene+plagioclase aggregates) suggests that the formation of plagioclase peridotites may be related to a reactive process, whereby a silica-oversaturated liquid crystallised plagioclase + orthopyroxene, while dissolving clinopyroxene and olivine. To test this hypothesis, we applied an AFC model, following the approach adopted by Rampone et al. (2008) for the impregnated peridotites from the Corsican ophiolites. The compositions of clinopyroxenes in equilibrium with the reacting melts with decreasing melt mass are plotted in Fig. 10. The same depleted liquids employed for the melt entrapment calculations displayed above are considered as reacting melts (see Fig. 10 for further explanations and modelling parameters). Impregnation by a boninite-like liquid yields clinopyroxenes with exceedingly low LREE-MREE-Ti contents, even for low residual melt mass (Fig. 10a). On the other hand, the whole range of

clinopyroxene compositions in plagioclase-bearing lherzolites (excepting Zr) may be reproduced using non-aggregated MORB melts (Fig. 10b).

The occurrence of impregnated plagioclase lherzolites in the New Caledonia mantle section reflects *in situ* melt entrapment at relatively shallow levels after polybaric melt extraction starting in the garnet stability field. The impregnation process at plagioclase-facies conditions most likely involves incremental melt fractions that survived unmixed before aggregation. In some alpine ophiolitic mantle sections, the impregnating melt is shown to have similar geochemical characteristics (e.g. Rampone et al., 2008; Piccardo and Guarnieri, 2012). In general, the formation of impregnated plagioclase peridotites has been related to stagnation of melts rising through the oceanic lithosphere in regions dominated by conductive cooling, e.g. oceanic transform faults (Seyler and Bonatti, 1997; Tartarotti et al., 2002), core complex megamullions (Dick et al., 2010; Loocke et al., 2013) or magma-poor margins (e.g. Müntener et al., 2010). The close association of the plagioclase lherzolites from the Poum massif with a major mylonitic shear zone, interpreted as an oceanic paleo-transform fault (Leblanc, 1995; Nicolas, 1989), may be consistent with a scenario of melt focusing along the shear zone, leading to melt stagnation and melt-rock reaction in the undeformed peridotites nearby.

8.3. Late-stage enrichment processes in bulk rock and clinopyroxene

The New Caledonia residual lherzolites display enrichments in the most incompatible trace elements (from Cs to Sr in the extended diagrams normalised to PM, Fig. 4-5) in both the bulk rock and constituent clinopyroxenes that cannot be accounted for by melting processes. These selective enrichments require different processes, possibly related to melt-rock or fluid-rock interaction.

In abyssal and ophiolitic residual peridotites the enriched signature of clinopyroxene may result from inefficiently extracted melt (Hellebrand et al., 2002; Niu, 2004, Brunelli et al., 2006). Nevertheless, the lack of textural evidence, i.e. interstitial, secondary clinopyroxene or thin films around primary mantle minerals (Seyler et al., 2001), does not support this hypothesis.

Alternatively, the cryptic enrichment shown by clinopyroxene can be driven by chromatographic processes related to percolation of small melt fractions into already depleted peridotites (Navon and Stolper, 1987; Godard et al., 1995; Vernières et al., 1997). Percolation may have occurred either during the sub-ridge evolution or during the subsequent involvement of the New Caledonia lherzolites in a convergent setting during Eocene (Aitchison et al., 1995a; Cluzel et al., 2001, 2012). Very low Th/Nb ratios (<0.05) recorded by clinopyroxene cores, however, tend to rule out an origin related to slab-derived melts in subduction setting (Dijkstra et al., 2009).

Bulk rock compositions are more enriched in Ba, Pb, Sr, La and Ce than clinopyroxenes (Fig. 4-5). As no textural evidence for modal metasomatism is discernible, the incompatible elements in "excess" may be be stored along grain boundaries, in small amounts of fluid/melt inclusions trapped in minerals (Garrido et al., 2000) or in secondary alteration minerals.

Addition of incompatible elements by the highly depleted melts involved in the formation of the plagioclase lherzolites (section 8.2) is unlikely. Overall, the lack of meaningful correlation with HFSE abundances rules out the possibility that selective increases of bulk-rock Ba, Pb, Sr, La and Ce contents are related to melt-rock interaction (Paulick et al., 2006). On the other hand, these elements are well known to be mobile during seafloor hydrothermal alteration (Paulick et al., 2006; Deschamps et al., 2010) and in subduction-related fluids (Bebout, 2014). We therefore propose that the fluid-mobile element enrichments, and the associated displacement of $^{87}Sr/^{86}Sr$ ratios towards radiogenic values is a result of low to moderate degrees of serpentinisation (Fig. 6), likely related to hydrothermal seafloor alteration. Although the role of subduction-related fluids cannot be ruled out from existing data, direct evidence for their involvement is lacking.

8.4. Isotopic constraints on the mantle sources

As shown in Fig. 6, most lherzolite samples have initial Sr isotopic compositionx well above 0.705 and display a subhorizontal trend in an Sr-Nd plot, showing increasing $^{87}Sr/^{86}Sr$ against slightly variable $^{143}Nd/^{144}Nd$. Similar

trends are commonly observed in peridotites affected by hydrothermal alteration (Cipriani et al., 2004; Bosch et al., 2004; Rampone and Hofmann, 2012), which shifts the Sr isotopic composition towards the radiogenic values of seawater. In contrast, Nd is unaffected by these alteration processes so that its isotope composition may be considered representative of its mantle source, even in highly serpentinised rocks.

Initial Nd isotope ratios of both spinel and plagioclase lherzolites are similar to the DMM composition (Fig. 6). The analysed samples have relatively homogeneous Nd isotope composition compared to the heterogeneity displayed by modern abyssal peridotites (Fig. 6). In addition, somewhat uniform $^{143}Nd/^{144}Nd$ ratios coupled with variable $^{147}Sm/^{144}Nd$ ratios (Fig. 11), suggest that the New Caledonia lherzolites represent a residual mantle source of asthenospheric origin that experienced a recent (MORB-producing?) depletion event (see also Rampone and Hofmann, 2012). Likewise, the young Nd model ages obtained for New Caledonia lherzolites (T_{DM} < 80 Ma, Table 2) indicate recent melting of a depleted asthenospheric source. We therefore propose that this event may be related to decompression melting in a marginal basin before the onset of Eocene subduction (Aitchison et al., 1995; Cluzel et al., 2001; Cluzel et al., 2012).

8.5. Crust-mantle relationships: assessment of a genetic link between Poya Terrane basalts and northern lherzolites

Based on a batch melting model, Ulrich et al. (2010) recently proposed that the melts extracted from the lherzolites were similar to the E-MORB basalts of the Poya terrane. In the light of our new trace element and Nd isotopic data, we re-examine this hypothesis. To this end, we have computed the REE composition of aggregated liquids derived from melting of a depleted mantle source (Table S5). The calculations were performed using the garnet-spinel fractional melting model which successfully explains the residual spinel lherzolite compositions (see section 8.1). The obtained liquids (Fig. 12a) were then compared with the Poya E-MORB. These basalts display flat LREE patterns and nearly flat to slightly positive MREE/HREE ratios, which argue for the

involvement of garnet in their sources (e.g. Hirschmann and Stolper, 1996). The calculated liquids formed after 4% of melting in the garnet stability field followed by 4-6% of melting in the spinel peridotite field have REE patterns characterised by flat to slightly depleted LREE and weakly fractionated MREE/HREE, subparallel to those of Poya E-MORBs, but at lower absolute concentrations. On the other hand, a smaller degree of garnet field melting (Fig. 12b) fails to reproduce the slight MREE enrichment over HREE exhibited by the Poya E-MORBs. On the whole, the modelling indicates that these basalts require a source more enriched in incompatible elements with respect to a typical MORB-type mantle.

The lherzolites from the Babouillat and Poum massifs and the Poya basalts display distinct Nd isotope compositions (Fig. 6). In particular, the lherzolites are characterized by age-corrected Nd isotope compositions significantly more radiogenic ($\varepsilon_{Nd(i)}$ from +6.98 to +10.97) than those shown by the Poya basalts ($\varepsilon_{Nd(i)}$ from +2.77 to +5.52, Cluzel et al., 2001 and this work).

In summary, geochemical trace element modelling and Nd isotopes do not seem to support a genetic mantle-crust link between Poya Terrane basalts and the New Caledonian lherzolites that underlie them.

Mantle-crust relations at oceanic settings is a debated issue. Radiogenic isotope studies have shown that abyssal and ophiolitic peridotites have more heterogeneous isotopic compositions than the crust to which they are related (e.g. Rampone and Hofmann, 2012; Mallick et al., 2014). Our findings are also consistent with the notion that abyssal peridotites are, on average, isotopically more depleted than MORB. Nd isotopic variability of the crustal rocks may reflect different proportions of variably depleted peridotite and the presence a low solidus component with a more enriched isotopic signature in the subridge melting region (Salters and Dick, 2002; Sobolev et al., 2007). We can therefore speculate that melting of mafic heterogeneities stored in the convecting mantle could have contributed to the enriched geochemical and Nd isotopic signature of the Poya E-MORB (Sobolev et al., 2007; Montanini et al., 2012). Hence, the lack of a simple residue-melt relationship does not preclude that the lherzolites were involved in the basalt petrogenesis, if a more

enriched, non-peridotitic component was present in the source. We conclude that geochemical data cannot unambiguosuly determine whether the lherzolites and the Poya basalts represented the oceanic lithosphere of a single marginal basin.

9. Summary and conclusions

In this work, we have carried out a geochemical investigation on the New Caledonia lherzolites, providing a comprehensive geochemical data set (major, trace element and Sr-Nd isotopes) on these rocks. Our study reconstructs the evolution of the peridotites from a recent event of melt extraction starting in the garnet stability field, to shallow level melt impregnation. Mantle-crust relationships in light of geochemical modelling and Nd isotope compositions were also discussed. Mineral and bulk rock geochemistry indicate that New Caledonia lherzolites represent moderately depleted residual peridotites with abyssal-type affinity. Bulk rock and clinopyroxene compositions of spinel lherzolites are consistent with moderate degrees of fractional melting of a DMM source (8-9%), including a first stage of deep melting in the presence of residual garnet. According to Sm-Nd isotope systematics, the lherzolites are derived from a relatively homogenous asthenospheric reservoir that experienced a recent depletion event. Plagioclase lherzolites are formed by post-melt extraction evolution of the depleted spinel lherzolites. Geochemical modelling suggests that plagioclase crystallised following trapping of highly depleted, incremental melt fractions of a MORB-type source.

The New Caledonia lherzolites record a history of partial melting in the asthenosphere, and subsequent melt–rock interaction at shallow, lithospheric depths. This evolution was likely related to seafloor spreading in a marginal basin predating Eocene subduction. Geochemical trace element modelling and Nd isotopes do not support a simple genetic mantle-crust link between the northern massif lherzolites and basaltic rocks with E-MORB affinity from the Poya terrane. These basalts require the presence of isotopically enriched material, possibly non-peridotitic, in their mantle source.

Acknowledgments

The authors are grateful to B. Galland, C. Douchet, O. Bruguier, P. Verdoux and P. Telouk for their expertise in chemical room management, ICP-MS, TIMS and MC-ICP-MS analyses, respectively. We are indebted to Daniele Brunelli (University of Modena) and Roberto Braga (University of Bologna) for XRF analyses. We thank P. Sossi (Institute de Physique du Globe de Paris) and S.L. Williams (University of Parma) for the revision of the English text. This paper is part of the PhD work of A.S. which was supported by a Vinci grant (Italian-French University).

References

Aitchison, J.C., Clarke, G.L., Meffre, S., Cluzel, D., 1995a. Eocene arc-continent collision in New Caledonia and implications for regional southwest Pacific tectonic evolution. Geology 23, 161–164.

Aitchison J.C., S. Meffre and D. Cluzel 1995b. Cretaceous/Tertiary radiolarians from New Caledonia, Geological Society of New Zealand Miscelaneous Publ. 81A, p. 7.

Albarede, F., 1996 Introduction to geochemical modelling. Cambridge University Press, p. 405.

Aldanmaz, E., Schmidt, M.V., Gourgaud, A., Meisel, T., 2009. Mid-ocean ridge and supra-subduction geochemical signatures in spinel–peridotites from the Neotethyan ophiolites in SW Turkey: Implications for upper mantle melting processes. Lithos, 113, 691-708.

Arai, S., 1994. Characterization of spinel peridotites by olivine-spinel compositional relationships: review and interpretation. Chemical Geology 113, 191-204.

Barth, M.G., Mason, P.R.D., Davies, G.R., Dijkstra, A.H., Drury, M.R., 2003. Geochemistry of the Othris Ophiolite, Greece: Evidence for Refertilization? Journal of Petrology 44, 1759-1785.

Bebout, G.E., 2014. Chemical and Isotopic Cycling in Subduction Zones. Treatise on Geochemistry, 703-747.

Bindeman, I.N., Davis, A.M., Drake, M.J., 1998. Ion microprobe study of plagioclase-basalt partition experiments at natural concentration levels of trace elements. Geochimica et Cosmochimica acta 62, 1175-1193.

Bosch, D., Jamais, M., Boudier, F., Nicolas, A., Dautria, J.M., Agrinier, P., 2004. Deep and high temperature hydrothermal circulation in the Oman ophiolite. Petrological and isotopic evidence. Journal of Petrology 45, 1181–1203.

Brey, G. P., Kohler, T., 1990. Geothermobarometry in four-phase lherzolites II. New thermobarometers, and practical assessment of existing thermobarometers. Journal of Petrology 31, 1353-1378.

Brunelli, D., Seyler, M., Cipriani, A., Ottolini, L., Bonatti, E., 2006. Discontinuous Melt Extraction and Weak Refertilization of Mantle Peridotites at the Vema Lithospheric Section (Mid-Atlantic Ridge). Journal of Petrology 47, 745-771.

Cannat, M., Juteau, T., Berger, E., 1990, Petrostructural analysis of the Leg 109 serpentinized peridotites, in Detrick, R., et al., Proceedings of the Ocean Drilling Program, Scientific results, Volume 106/109: College Station, Texas, Ocean Drilling Program, 47–57.

Chauvel, C., Blichert-Toft, J., 2001. A hafnium isotope and trace element perspective on melting of the depleted mantle. Earth and Planetary Science Letters 190, 137-151.

Chazot, G., Charpentier, S., Kornprobst, J., Vannucci, R., Luais, B., 2005. Lithospheric mantle evolution during continental break-up: the West Iberia non-volcanic passive margin. Journal of Petrology 46, 2527–2568.

Choi, S.H., Shervais, J.W., Mukasa, S.B., 2008. Supra-subduction and abyssal mantle peridotites of the Coast Range ophiolite, California. Contributions to Mineralogy and Petrology 156, 551-576.

Cipriani, A., Brueckner, H.K., Bonatti, E., Brunelli, D., 2004. Oceanic crust generated by elusive parents: Sr and Nd isotopes in basalt-peridotite pairs from the Mid-Atlantic Ridge. Geology 32, 657-660.

Cluzel, D., Aitchison, J., Clarke, G., Meffre, S., Picard, C., 1994. Point de vue sur l'évolution tectonique et géodynamique de la Nouvelle-Calédonie. Comptes Rendus de l'Academie des Sciences de Paris 319, 683-688.

Cluzel, D., Aitchison, J. et Picard, C., 2001. Tectonic accretion and underplating of mafic terranes in the Late Eocene intraoceanic fore-arc of New Caledonia (Southwest Pacific): geodynamic implications. Tectonophysics 340, 23-59.

Cluzel D., Jourdan F., Meffre S., Maurizot P., Lesimple S., 2012. The metamorphic sole of New Caledonia ophiolite: $^{40}Ar/^{39}Ar$, U-Pb, and geochemical evidence for subduction inception at a spreading ridge. Tectonics 31, 17-27.

Cluzel, D., Chiron, D., Courme, M.D., 1998. Discordance de l'Eocène supérieur et événements pré-obduction en Nouvelle-Calédonie (Pacifique sud-ouest). Comptes rendus de l'Académie des sciences. Série 2. Sciences de la terre et des planètes 327, 485-91.

Cluzel, D., Picard, C., Aitchison, J., Laporte, C., Meffre, S., Parat, F., 1997. La nappe de Poya (ex-formation des basaltes) de Nouvelle Caldonie (Pacifique Sud-Ouest): un plateau océanique Campanien-Paléocène Supérieur obducté à l'Eocène supérieur. C. R. Acad. Sci., Pans 324, 443-451, Sér.IIa.

Cluzel, D., Meffre, S., Maurizot, P., Crawford, A.J., 2006. Earliest Eocene (53 Ma) convergence in the Southwest Pacific: evidence from pre-obduction dikes in the ophiolite of New Caledonia. Terra Nova 18, 395-402.

Collot, J.Y., Malahoff, A., Récy, J., Latham, G., Missegue, F., 1987. Overthrust emplacement of New Caledonia ophiolite: geophysical evidence. Tectonics 6, 215–232.

De Paolo, D.J, 1981. Trace elements and isotopic effects of combined wall rock assimilation and fractional crystallization. Earth and Planetary Science Letters 53, 189–202.

Deschamps, F., Guillot, S., Godard, M., Chauvel, C., Andreani, M., Hattori, K., 2010. In situ characterization of serpentinites from forearc mantle wedges: Timing of serpentinization and behavior of fluid-mobile elements in subduction zones. Chemical Geology 269, 262–277.

Dick, H.J.B., Bullen, T., 1984. Chromian spinel as a petrogenetic indicator in abyssal and alpine-type peridotites and spatially associated lavas. Contributions to Mineralogy and Petrology 86, 54–76.

Dick, H.J.B., Lissenberg, C. J. and Warren, J.M., 2010. Mantle melting, melt transport and delivery beneath a slow-spreading ridge: The paleo-MAR from 238150 N to 238450 N. Journal of Petrology 50, 425-467.

Dijkstra, A.H., Sergeev, D.S., Spandler, C., Pettke, T., Meisel, T., Cawood, P.A., 2010. Highly Refractory Peridotites on Macquarie Island and the Case for Anciently Depleted Domains in the Earth's Mantle. Journal of Petrology 51, 469-493.

Dilek, Y. and Furnes, H., 2011. Ophiolite genesis and global tectonics: Geochemical and tectonic fingerprinting of ancient oceanic lithosphere. Geological Society of America bulletin 123, 387-411.

Dupuy, C., Dostal, J., Leblanc, M., 1981. Geochemistry of an ophiolitic complex from New Caledonia. Contributions to Mineralogy and Petrology 76, 77-83.

Eisele, J., Sharma, M., Galer, S.J.G., Blichert-Toft, J., Devey, C.W., Hofmann, A.W., 2002. The role of sediment recycling in EM-1 inferred from Os, Pb, Hf, Nd, Sr isotope and trace element systematics of the Pitcairn hotspot. Earth Planetary Science Letters 196, 197–212.

Eissen, J.-P., Crawford, A.J., Cotten, J., Meffre, S., Bellon, H., Delaune, M., 1998. Geochemistry and tectonic significance of basalts in the Poya Terrane, New Caledonia. Tectonophysics, 203–219.

Elthon, D., 1992. Chemical trends in abyssal peridotites: re-fertilization of depleted suboceanic mantle. Journal of Geophysical Research 97, 9015-9025.

Garrido, C.J., Bodinier, J.L., Alard, O., 2000. Incompatible trace element partitioning and residence in anhydrous spinel peridotites and websterites from the Ronda orogenic peridotite. Earth and Planetary Science Letters 181, 341-358.

Godard, M., Bodinier, J.L., Vasseur, G., 1995. Effects of mineralogical reactions on trace element redistributions in mantle rocks during percolation processes: A chromatographic approach. Earth and Planetary Science Letters 133, 449-461.

Hamelin, B., Dupré, B., Allègre, C.J., 1984. The lead isotope systematics of ophiolite complexes. Earth and Planetary Science Letters 67, 351-366.

Hellebrand, E., Snow, J.E., Dick, H.J.B., Hofmann, A.W., 2001. Coupled major and trace elements as indicators of the extent of melting in mid-ocean-ridge peridotites. Nature 410, 677-681.

Hellebrand, E., Snow, J. E., Hoppe, P., Hofmann, A. W., 2002. Garnet-field Melting and Late-stage Refertilization in 'Residual' Abyssal Peridotites from the Central Indian Ridge. Journal of Petrology 43, 2305-2338.

Hirschmann, M.M., Stolper, E.M., 1996. A possible role for garnet pyroxenite in the origin of the garnet signature in MORB. Contributions to Mineralogy and Petrology 124, 185-208.

Hofmann, A.W., 2003. Sampling Mantle Heterogeneity through Oceanic Basalts: Isotopes and Trace Elements. In: Carlson, R.W. (Ed.), Treatise on Geochemistry 2, The mantle and core, pp. 61–101.

Johnson, K., Dick, H.J.B., Shimizu, N., 1990. Melting in the oceanic upper mantle: an ion microprobe study of diopsides in abyssal peridotites. Journal of Geophysical Research 95, 2661-2678.

Johnson, K.T.M. and Dick, H.J.B., 1992. Open system melting and temporal and spatial variation of peridotite and basalt at the Atlantis II fracture zone. Journal of Geophysical Research 97, 9219-9241.

Kaczmarek, M.A. and Müntener, O. (2008). Juxtaposition of melt impregnation and high-temperature shear zones in the upper mantle; field and petrological constraints from the Lanzo peridotite (Northern Italy). Journal of Petrology 49, 2187-2220.

Kempton, P.D. and Stephens, C.J., 1997. Petrology and geochemistry of nodular websterite inclusions in harzburgite, hole 920D. In: Karson, J.A., Cannat, M., Miller, D.J., Elthon, D. (Eds.), Proceeding of Ocean Drilling Program, Scientific Results 153. Ocean Drilling Program, College Station, TX, 321–331.

Kinzler, R.J., 1997. Melting of mantle peridotite at pressures approaching the spinel to garnet transition: Application to mid-ocean ridge basalt petrogenesis. Journal of Geophysical Research 102, 853 – 874

Klemme, S., 2004. The influence of Cr on the garnet–spinel transition in the Earth's mantle: experiments in the system $MgO–Cr_2O_3–SiO_2$and thermodynamic modelling. Lithos 77, 639-644.

Ionov, D.A., Savoyant, L., Dupuy, C., 1992. Application of the ICP-MS technique to trace element analysis of peridotites and their minerals. Geostandards Newsletters 16, 311–315.

Ionov, D.A., Bodinier J.L., Mukasa, S.B., Zanetti, A., 2002. Mechanisms and sources of mantle metasomatism: major and trace element compositions of peridotite xenoliths from Spitsbergen in the context of numerical modelling. Journal of Petrology 43, 2219-2259.

Ishii, T., Robinson, P.T., Mackawa, H., Fiske, R., 1992. Petrological studies of peridotites from diapiric serpentinite seamounts in the Izu-Ogazawara-Mariana forearc, LEG 125. Proceedings of Ocean Drilling Program, Scientific Results 125, 445–485.

Lagabrielle, Y., Chauvet, A., Ulrich, M., Guillot, S., 2013. Passive obduction and gravity-driven emplacement of large ophiolitic sheets: The New Caledonia ophiolite (SW Pacific) as a case study? Bulletin de la Société Géologique de France 184, 545-556.

LaTourrette, T.Z., Kennedy, A.K., Wasserburg G.J., 1993. Thorium-Uranium factionation by garnet: evidence for a deep source and rapid rise of oceanic basalts . Science 261, 739-742.

Leblanc ,M.,1995. Chromitite and ultramafic rock compositional zoning through a paleotransform fault, Poum, New Caledonia. Economic Geology 90, 2028-2039.

Loocke, M., Snow, J.E., Ohara, Y., 2013. Melt stagnation in peridotites from the Godzilla Megamullion Oceanic Core Complex, Parece Vela Basin, Philippine Sea. Lithos 182–183, 1–10.

Mallick, S., Dick, H.J.B., Sachi-Kocher, A., Salters V.J.M., 2014. Isotope and trace element insights into heterogeneity of subridge mantle. Geochemistrym Geophysics, Geosystems 15, doi:10.1002/2014GC005314.

Marchesi, C., Garrido, C.J., Godard, M., Belley, F., Ferré, E., 2009. Migration and accumulation of ultra-depleted subduction-related melts in the Massif du Sud ophiolite (New Caledonia). Chemical Geology 266, 180-195.

McDonough, W.F., Stosch, H.G., Ware, N.G., 1992. Distribution of titanium and the rare earth elements between peridotitic minerals. Contributions to Mineralogy and Petrology 110, 321-328.

McDonough, W.F., Sun, S.S., 1995. The composition of the Earth. Chemical Geology 120, 223-253.

Miyashiro, A., 1973. The Troodos ophiolitic complex was probably formed in an island arc. Earth and Planetary Science Letters 19, 218-224.

Montanini, A., Tribuzio, R., Thirlwall, M., 2012. Garnet clinopyroxenite layers from the mantle sequences of the Northern Apennine ophiolites (Italy): Evidence for recycling of crustal material. Earth and Planetary Science Letters 351-352, 171-181.

Müntener, O., Pettke, T., Desmurs, L., Meier, M., Schaltegger, U., 2004. Refertilization of mantle peridotite in embryonic ocean basins: trace element and Nd isotopic evidence and implications for crust-mantle relationships. Earth and Planetary Science Letters 221, 293-308.

Müntener, O., Manatschal, G., Desmurs, L., Pettke, T., 2010. Plagioclase peridotites in ocean-continent transitions: refertilized mantle domains generated by melt stagnation in the shallow mantle lithosphere. Journal of Petrology 51, 255-294.

Navon, O., Stolper, E. , 1987. Geochemical consequences of melt percolation: the upper mantle as a chromatographic column. Journal of Geology 95, 285-307.

Nicolas, A. and Dupuy, C., 1984. Origin of ophiolite and oceanic lherzolites. Tectonophysics 110, 177–187.

Nicolas A., Prinzhofer A., 1983. Cumulative or residual origin for the transition zone in ophiolites: structural evidence. Journal of Petrology 24, 188–206.

Nicolas, A., 1989. Structures of ophiolites and dynamics of oceanic lithosphere. Kluwer, Dordrecht, 368 pp.

Niu, Y., 1997. Mantle melting and melt extraction processes beneath ocean ridges: evidence from abyssal peridotites. Journal of Petrology 38, 1047–1074.

Niu, Y., 2004. Bulk-rock Major and Trace Element Compositions of Abyssal Peridotites: Implications for Mantle Melting, Melt Extraction and Post-melting Processes Beneath Mid-Ocean Ridges. Journal of Petrology 45, 2423-2458.

O'Neill, 1981. The transition between spinel lherzolite and garnet lherzolite, and its use as a Geobarometer. Contributions to Mineralogy and Petrology 77, 185-194.

Palmer, M.R., Edmond, J.M., 1989. The strontium isotope budget of the modern ocean. Earth Planetary Science Letters 92, 11–26.

Paulick, H., Bach, W., Godard, M., De Hoog, J.C.M., Suhr, G., Harvey, J., Geochemistry of abyssal peridotites (Mid-Atlantic Ridge, 15°20'N, ODP Leg 209): Implications for fluid/rock interaction in slow spreading environments. Chemical Geology 234, 179-210.

Pearce, J.A., Lippard, S.J. and Roberts, S., 1984. Characteristics and tectonic significance of supra-subduction zone ophiolites. In: Kokelaar, P. B. and Howells, M. F. (eds) Marginal Basin Geology. Geological Society, London, Special Publications 16, 77-94.

Pearce, N.J., Perkins, W.T., Westgate, J.A., Gorton, M.P., Jackson, S.E., Neal, C.R., Chenery, S.P., 1997. A compilation of new and published major and trace element data for NIST SRM 610 and NIST SRM 612 glass reference materials. Geostandards Newsletter 21, 115–144.

Pearce, J. A., Barker, P. F., Edwards, S. J., Parkinson, I. J. and Leat, P.T., 2000. Geochemistry and tectonic significance of peridotites from the South Sandwich arc-basin system, South Atlantic. Contributions to Mineralogy and Petrology 139, 36-53.

Piccardo, G.B., Zanetti, A., Müntener, O., 2007. Melt/peridotite interaction in the Southern Lanzo peridotite: Field, textural and geochemical evidence. Lithos 94, 181-209.

Piccardo, G.B., and Guarnieri, L. (2012). The Monte Maggiore peridotite (Corsica, France): a case study of mantle evolution in the Ligurian Tethys. In: Coltorti, M., Downes, H., Gregoire, M. and O'Reilly, S. Y. (eds) Petrological

Evolution of the European Lithospheric Mantle. Geological Society, London, Special Publications, 337, 7–45

Piepgras, D.J., Wasserburg, G.J., 1987. Rare-earth element transport in the western North- Atlantic inferred from Nd isotopic observations. Geochimica et Cosmochimica Acta 51, 1257–1271.

Pin, C., Briot, D.,Bassin, C.,Poitrasson, F., 1994. Concomitant separation of strontium and samarium–neodymium for isotopic analysis in silicate samples, based on specific extraction chromatography. Analytica Chimica Acta 298, 209–217.

Pirard, C., Hermann, J., O' Neill, H.St.C., 2013. Petrology and Geochemistry of the Crust-Mantle Boundary in a Nascent Arc, Massif du Sud Ophiolite, New Caledonia, SW Pacific. Journal of Petrology 0, 1-34.

Prinzhofer, A., Nicolas, A., Cassard, D., Moutte, J., Leblanc, M., Paris, J.M., Rabinovitch, M., 1980. Structures in the New Caledonia peridotites-gabbros: Implications for oceanic mantle and crust. Tectonophysics 69, 85-112.

Prinzhofer, A., Allegre, C. J., 1985. Residual peridotites and the mechanisms of partial melting. Earth and Planetary Science Letters 74, 251-265.

Rampone, E., Bottazzi, P., Ottolini, L., 1991. Complementary Ti and Zr anomalies in orthopyroxene and clinopyroxene from mantle peridotites. Nature 354, 518-520.

Rampone, E., Piccardo, G.B., Vannucci, R., Bottazzi, P., Ottolini, L. (1993). Subsolidus reactions monitored by trace element partitioning: the spinel- to plagioclase-facies transition in mantle peridotites. Contributions to Mineralogy and Petrology 115, 1-17.

Rampone, E., Hoffman, A.W., Piccardo, G., Vannucci, R., 1995. Petrology, Mineral and Isotope Geochemistry of the External Liguride Peridotites (Northern Apennines, Italy). Journal of Petrology 36, 81-105.

Rampone, E., Piccardo, G.B., Hofmann, A.W., 2008. Multi-stage melt–rock interaction in the Mt. Maggiore (Corsica, France) ophiolitic peridotites: microstructural and geochemical evidence. Contributions to Mineralogy and Petrology 156, 453-475.

Rampone, E., Hofmann, A.W., 2012. A global overview of isotopic heterogeneities in the oceanic mantle. Lithos 148, 247–261.

Rodgers, K.A., 1975. Lower Tertiary tholeiitic basalts from southern New-Caledonia. Mineralogical Magazine 40, 25-32.

Routhier, E., 1953. Etude geologique du versant occidental de la Nouvelle-Calddonie entre le col de Boghen et la pointe d'Arama. Mémoires de la Société géologique de France: Nouvelle série, 322, 122-133.

Salters V.J.M., Stracke A., 1989. The hafnium paradox and the role of garnet in the source of mid-ocean-ridge basalts. Nature 342, 420-422.

Salters, V.J.M., Shimizu, N., 1988. World-wide occurrences of HFSE-depleted mantle. Geochimica et Cosmochimica Acta 52, 2177-2182.

Salters, V.J.M., Dick, H.J.B., 2002. Mineralogy of the mid-ocean-ridge basalt source from neodymium isotopic composition of abyssal peridotites. Nature 418, 68-72.

Salters, V.J.M., Stracke, A., 2004. Composition of the depleted mantle. Geochemistry Geophysics Geosystems 5, DOI: 10.1029/2003GC000597.

Saccani, E. and Photiades, A. , 2004. Mid-ocean ridge and supra-subduction affinities in the Pindos ophiolites (Greece): implications for magma genesis in a forearc setting. Lithos 73, 229-253.

Sécher, D., 1981. Les lherzolites ophiolitiques de la Nouvelle–Calédonie et leurs gisements de chromites, Université de Nantes, Nantes, 300pp.

Seyler, M., Bonatti, E., 1997. Regional-scale melt–rock interaction in lherzolitic mantle in the Romanche fracture zone, Atlantic Ocean. Earth and Planetary Science Letters 146, 273–287.

Seyler, M., Toplis, M.J., Lorand, J.P., Luguet, A., Cannat, M., 2001. Clinopyroxene microtextures reveal incompletely extracted melts in abyssal peridotites. Geology 29, 155-158.

Shervais, J.W., 2001. Birth, death, and resurrection: the life cycle of suprasubduction zone ophiolites. Geochemistry Geophyiscs Geosystems 2 2000GC000080, ISSN:1525-2027.

Snow, J.E., Hart, S.R., Dick, H.J.B., 1994. Nd and Sr isotope evidence linking mid-ocean ridge basalts and abyssal peridotites. Nature 371, 57–60.

Sobolev, A.V., Hofmann, A.W., Kuzmin, D.W., 2007. The amount of recycled crust in sources of mantle-derived melts. Science 316, 412–417.

Sun, S.S., McDonough, W.F., 1989. Chemical and isotopic systematics of oceanic basalts: implications for mantle composition and processes. Geological Society, London, Special Publications 42, 313-345.

Tachikawa, K., Jeandel, C., Roy-Barman, M., 1999. A new approach to the Nd residence time in the ocean: the role of atmospheric inputs. Earth Planetary Science Letters 170, 433–446.

Takahashi, E. and Kushiro, I., 1983. Melting of a dry peridotite at high pressures and basalt magma genesis. American Mineralogist 68, 859–879.

Tartarotti P., Susini S., Nimis P. and Ottolini L., 2002. Melt migration in the upper mantle along 1098 the Romanche Fracture Zone (Equatorial Atlantic). Lithos 63, 125-149.

Titus S.J., Maes S.M., Benford B., Ferré E.C., Tikoff B. 2011. Fabric development in the mantle section of a paleotransform fault and its effect on ophiolite obduction, New Caledonia. Lithosphere 3, 221-244.

Ulrich, M., Picard, C., Guillot, S., Chauvel, C., Cluzel, D., Meffre, S., 2010. Multiple melting stages and refertilization as indicators for ridge to subduction formation: The New Caledonia ophiolite. Lithos 115, 223- 236.

Vernières, L., Godard, M., Bodinier, J.L., 1997. A plate model for the simulation of trace element fractionation during partial melting and magma transport in the Earth's upper mantle. Journal of Geophysical Research 102, 24771-24784.

Vitale Brovarone, A., Agard, P., 2013. True metamorphic isograds or tectonically sliced metamorphic sequence? New high-spatial resolution petrological data for the New Caledonia case study. Contributions to Mineralogy and Petrology 166, 451-469.

Warren, J.M., Shimizu, N., Sakaguchi, C., Dick, H.J.B., Nakamura, E., 2009. An assessment of upper mantle heterogeneity based on abyssal peridotite isotopic compositions. Journal of Geophysical Research 114, B12203.

Webb, S.A.C., Wood, B.J., 1986. Spinel-pyroxene-garnet relationships and their dependence on Cr/Al ratio. Contributions to Mineralogy and Petrology 92, 471-480.

Wells, P.R.A., 1977. Pyroxene thermometry in simple and complex systems. Contributions to Mineralogy and Petrology 62, 129-139.

Whattam, S.A., 2009. Arc-continent collisional orogenesis in the SW Pacific and the nature, source and correlation of emplaced ophiolitic nappe components. Lithos 113, 88-114.

Zindler, A., Hart, S.R., 1986. Chemical geodynamics. Annual Review of Earth and Planetary Sciences 14, 493–571.

Figure captions

Fig. 1. Simplified geological map of New Caledonia (modified after Cluzel et al., 2001 and Vitale Brovarone and Agard, 2013). Location of the northern Lherzolite Massifs and the main sampling areas are also shown.

Fig. 2. Compositional variations of spinel: (a) Cr#-Mg#. Field for abyssal and fore-arc peridotites are taken from Dick and Bullen (1984) and Ishii et al. (1992), respectively; (b) Average olivine Mg# and spinel Cr# for spinel and plagioclase lherzolites. The olivine-spinel mantle array (OSMA) is shown by dashed lines. Field for supra-subduction zone, abyssal and passive margins peridotites after Dick and Bullen (1984), Arai (1994) and Pearce et al. (2000). Data for the New Caledonia harzburgites are from Secchiari (unpublished PhD thesis data); (c) Cr#-TiO_2 (wt.%). Spinel data from impregnated ophiolitic plagioclase lherzolites (Lower Platta: Müntener et al., 2010; Lanzo: Piccardo et al., 2007; External Ligurides: Rampone et al., 1995) are also shown for comparison.

Fig. 3. Bulk rock abundances of CaO, Al_2O_3, SiO_2 and FeO_t vs. MgO (data on anhydrous basis in wt.%), for New Caledonia spinel and plagioclase peridotites compared with calculated trends for residual peridotites using the model of Niu (1997). Source end-member is from McDonough and Sun (1995). Dashed lines: melting curves for isobaric batch melting; thick curves: near fractional melting.

Fig. 4. (a) Chondrite-normalised REE patterns for spinel and plagioclase lherzolites. Normalising values after Sun and McDonough (1989); (b) Primitive

mantle-normalised trace element patterns of New Caledonia spinel and plagioclase lherzolites. Normalising values after Sun and McDonough (1989).

Fig. 5. (a) Chondrite-normalised REE compositions of clinopyroxenes from spinel and plagioclase lherzolites. Shaded field represent clinopyroxene from abyssal peridotites (Johnson et al. 1990). Normalising values after Sun and McDonough (1989); (b) Primitive mantle-normalised trace element patterns of clinopyroxene from spinel and plagioclase lherzolites.

Fig. 6. $^{143}Nd/^{144}Nd$ versus $^{87}Sr/^{86}Sr$ diagram for lherzolites and Poya basalts. Age-corrected isotopic ratios have been plotted. Sr and Nd seawater isotopic compositions are taken from Palmer and Edmond (1989), Piepgras and Wasserburg (1987), Tachikawa et al. (1999). DMM, EMI, EMII and HIMU after Zindler and Hart (1986) and Eisele et al. (2002). The field of Pacific arcs includes Izu-Bonin, Tonga, Mariana and Solomon arcs (source: Georoc database http://georoc.mpch-mainz.gwdg.de/georoc/)

Fig. 7. Results of fractional melting modelling in the spinel stability field. (a) Chondrite-normalised REE patterns for whole rock residues formed by fractional melting of a spinel peridotite (light grey). Numbers next to grey lines are the degrees of melting. DMM= Depleted MORB Mantle (Salters and Stracke, 2004). Melting modes and crystal/liquid partition coefficients are reported in Table S5; (b) Chondrite-normalised REE patterns for residual clinopyroxenes after different degrees of fractional melting. DMM clinopyroxene after Hirschmann and Stolper (1996).

Fig. 8. Results of fractional melting modelling in the garnet and spinel stability fields for clinopyroxene. All data are chondrite-normalized. DMM Cpx after Hirschmann and Stolper (1996).

Fig. 9. Plagioclase-facies impregnation models showing chondrite-normalised REE-Zr-Y-Ti abundances of clinopyroxenes calculated for variable trapped melt modes in a spinel lherzolite (sample BA1), followed by trace element redistribution in a plagioclase-bearing assemblage (sample BAB2A, observed mode: olivine = 58.9 vol% orthopyroxene = 19.2 vol %, clinopyroxene = 10.7

vol %, spinel = 0.9 vol %, plagioclase = 10.2 vol%). The calculated clinopyroxenes are compared with those analysed in the plagioclase lherzolite BAB2A. The impregnating liquids were (a) a boninite-like melt, i.e. putative liquid in equilibrium with the average composition of clinopyroxene in the most primitive gabbronorites from the New Caledonia ophiolite (Secchiari PhD thesis, unpublished data), (b) a highly depleted MORB melt formed by fractional melting of a depleted spinel peridotite (degree of melting = 8%). Details of partial melting model and crystal/liquid partition coefficients adopted for the the calculations are reported in Table S5.

Fig. 10. Plagioclase-facies impregnation models showing chondrite-normalised REE-Zr-Y-Ti abundances of clinopyroxenes in equilibrium with trapped melts modified by assimilation-fractional crystallisation processes (AFC, De Paolo, 1981) at decreasing melt mass. The calculated clinopyroxenes are compared with the range of clinopyroxene compositions analyzed in the plagioclase lherzolites (shaded field). Following Rampone et al. (2008), the model assumes that the impregnating melts assimilate olivine and clinopyroxene (Ma = 50% ol + 50% cpx) and crystallise plagioclase and orthopyroxene (Mc = 70 % plagioclase + 30 % orthopyroxene). Assumed assimilation rate R (= Ma/Mc) is 0.7. The impregnating liquids were (a) a boninite-like melt and (b) a depleted MORB (see Fig. 10 for further details about the melt calculations). The composition of assimilated clinopyroxene is taken from the spinel peridotite POU2 (average of clinopyroxenes reported in Table S4); the composition of assimilated olivine has been calculated in equilibrium with clinopyroxene using crystal/liquid partition coefficients for clinopyroxene and olivine reported in Table S5.

Fig. 11. Present-day $^{143}Nd/^{144}Nd$ vs. $^{147}Sm/^{144}Nd$ values for New Caledonia lherzolites. $^{143}Nd/^{144}Nd$ variation defined by > 90% global MORB (Warren et al., 2009) is also shown for comparison. Data for SWIR (Atlantis II Fracture Zone and Oblique Segment) and MAR (Mid Atlantic ridge) peridotites are from Snow et al. (1994), Kempton & Stephens (1997), Salters and Dick (2002), Cipriani et al. (2004), Chazot et al. (2005), Warren et al. (2009),

Fig. 12. Chondrite-normalised REE compositions of aggregated melts in equilibrium with a depleted spinel peridotite source compared with Poya E-MORB (Cluzel et al., 2001, shaded area and this work). Modelled melts obtained by 4 % (a) and 2% (b) of garnet facies melting plus 4-6% spinel facies melting. Mantle source composition, melting model parameters and crystal/liquid partition coefficients are reported in Table S5.

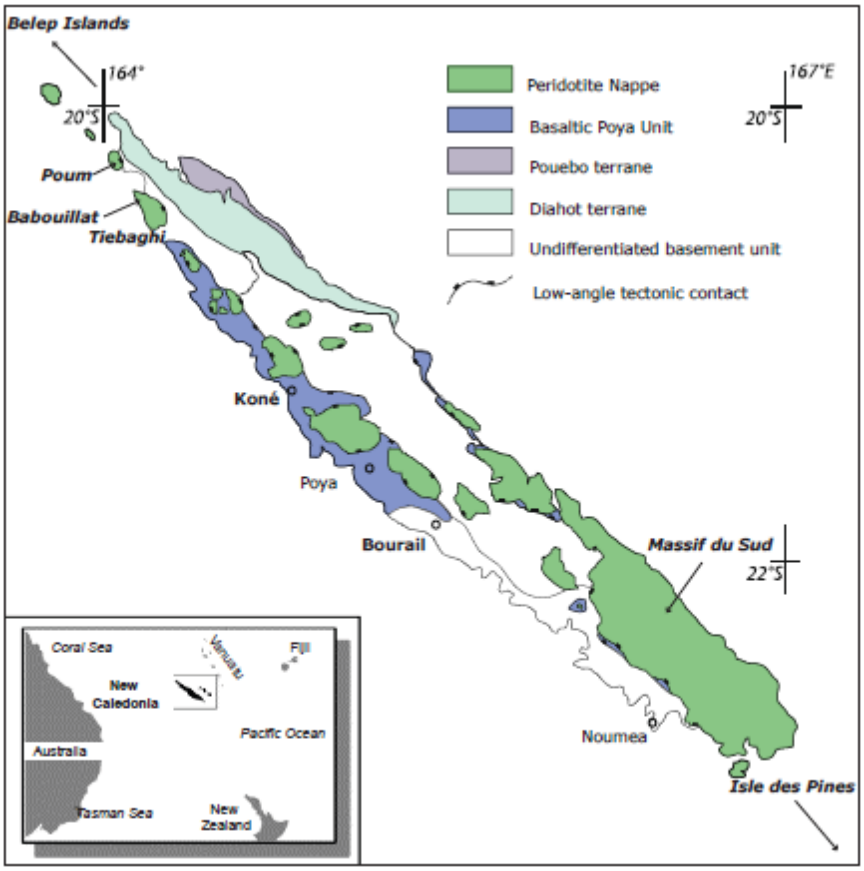

Fig. 1

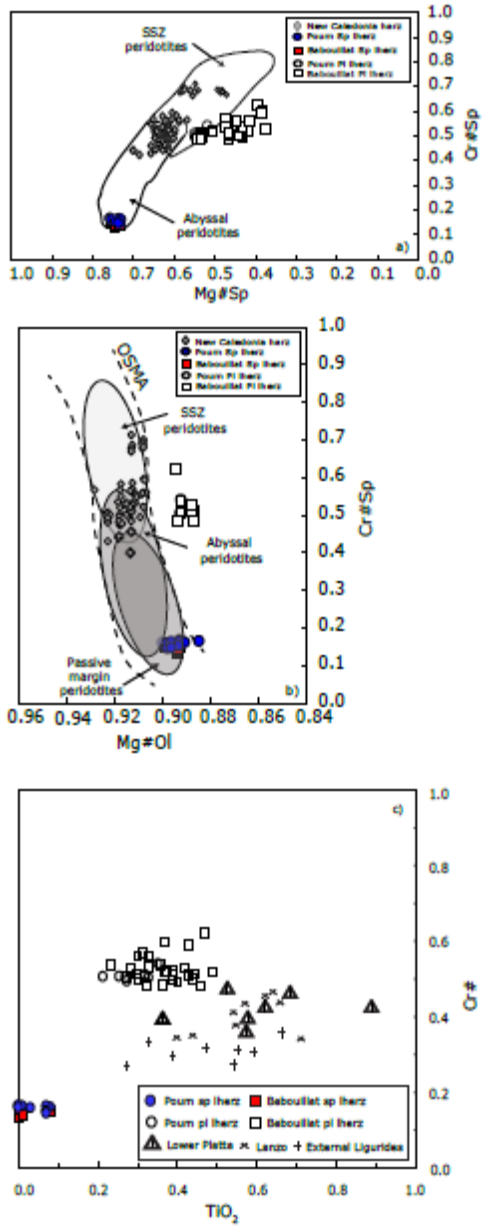

Fig. 2

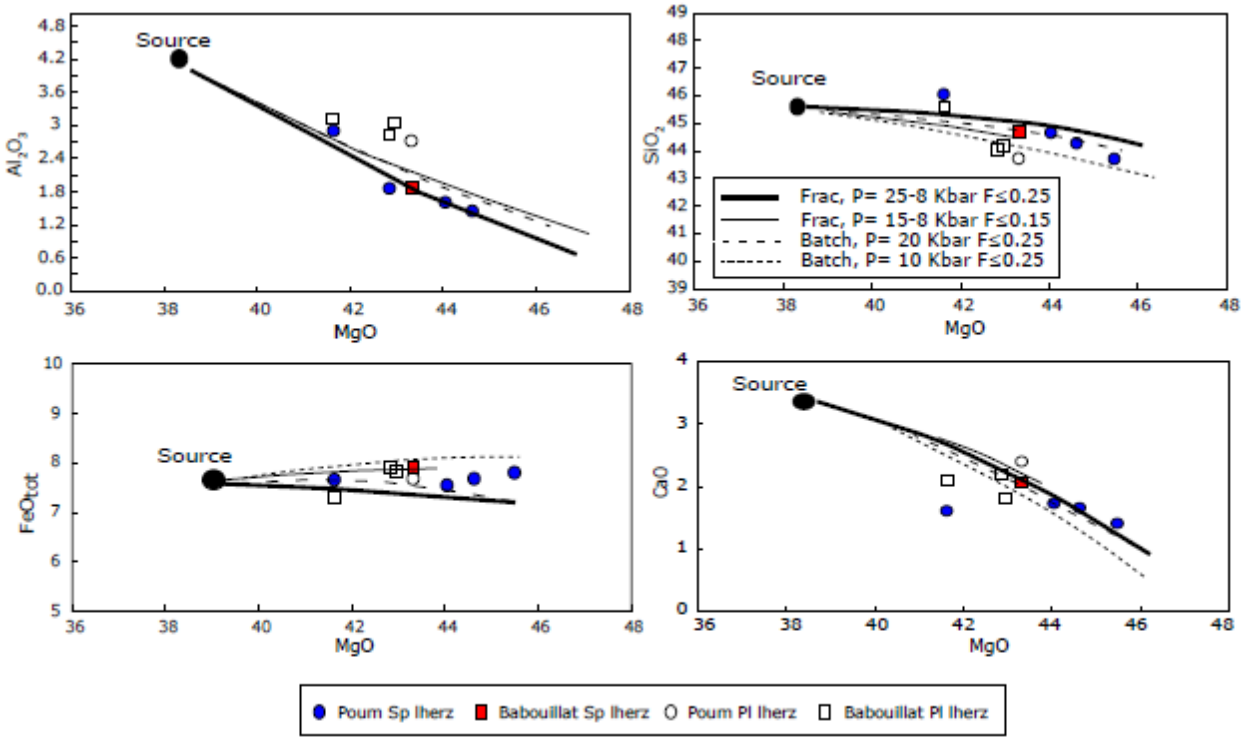

Fig. 3

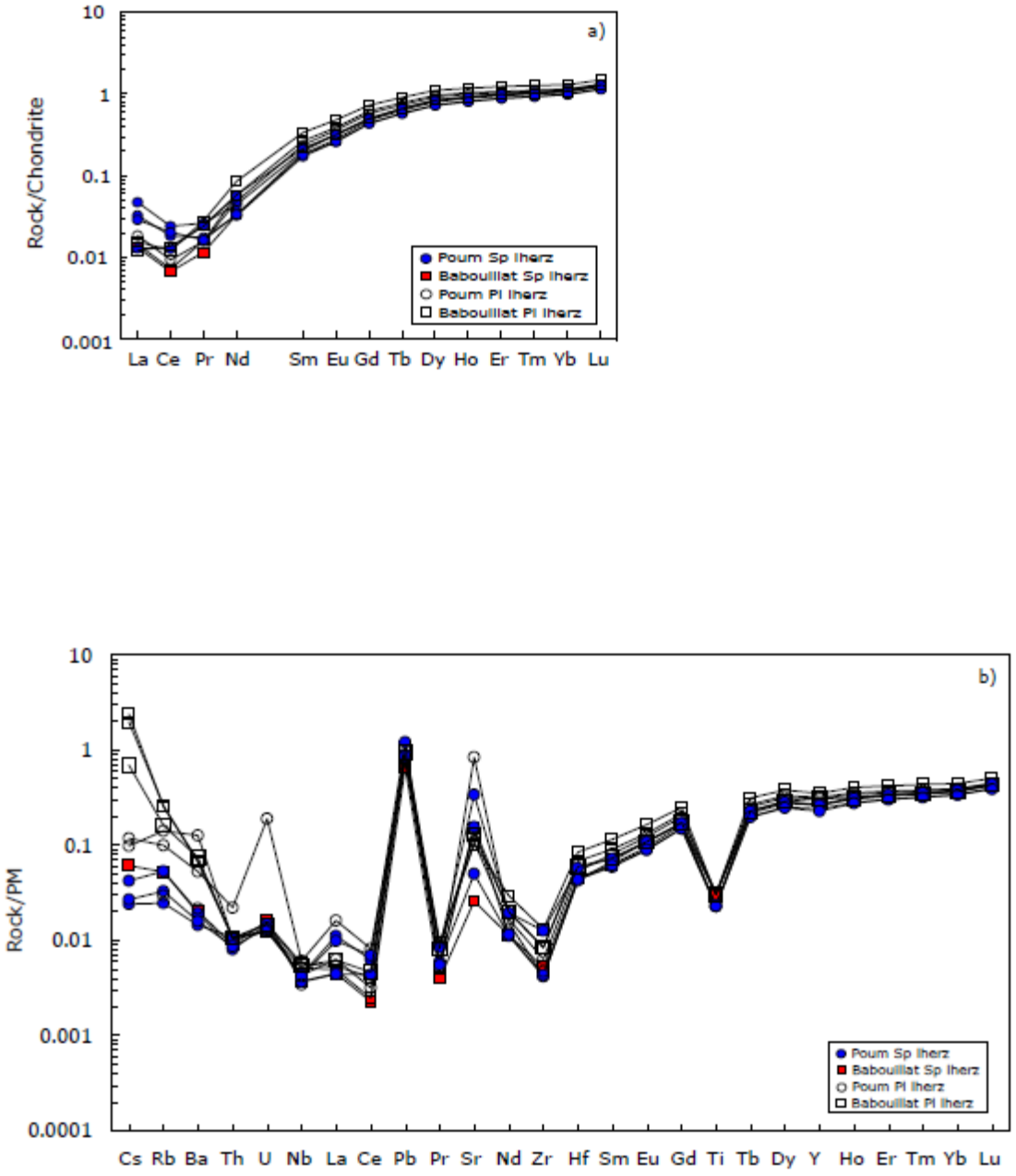

Fig. 4

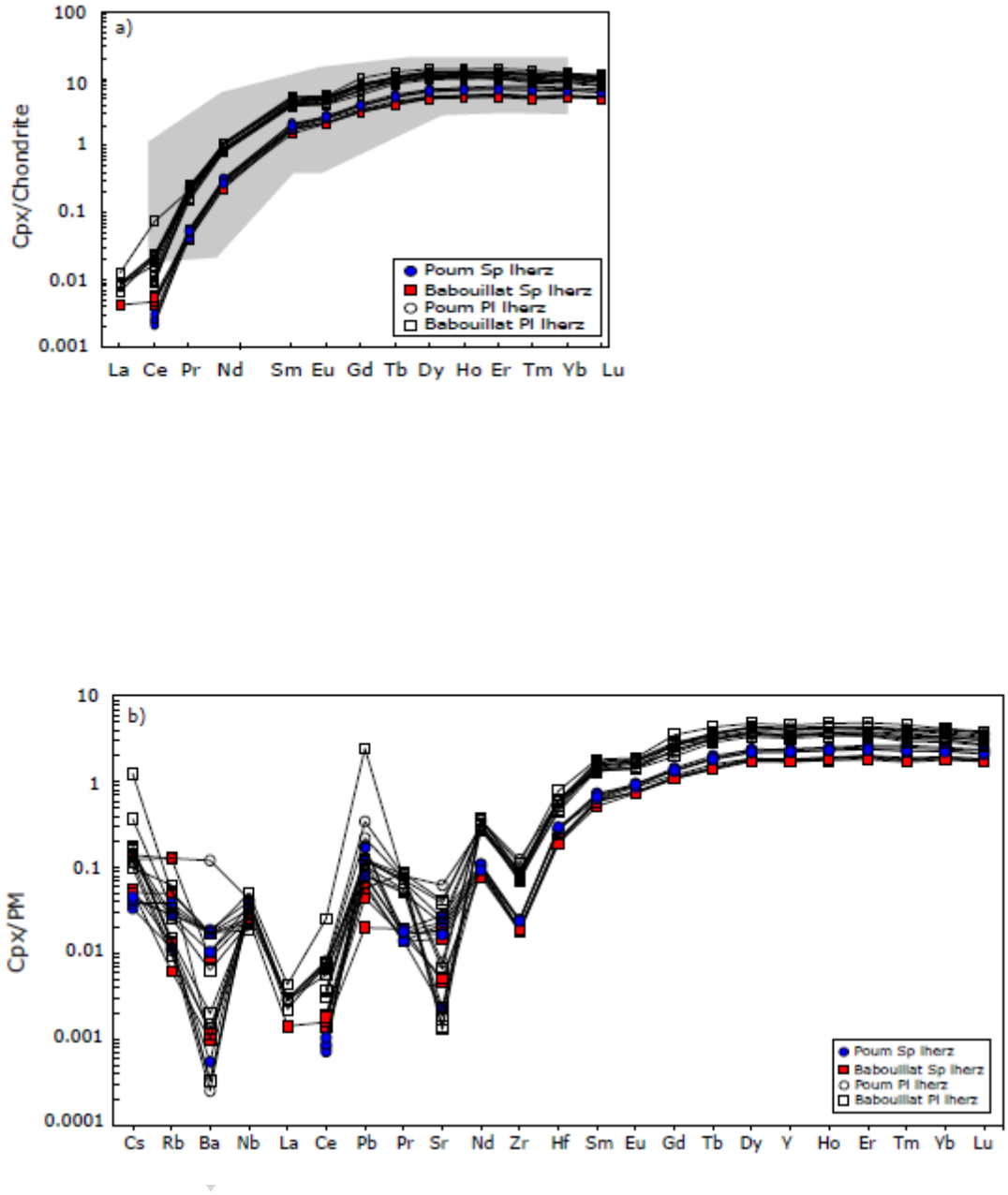

Fig. 5

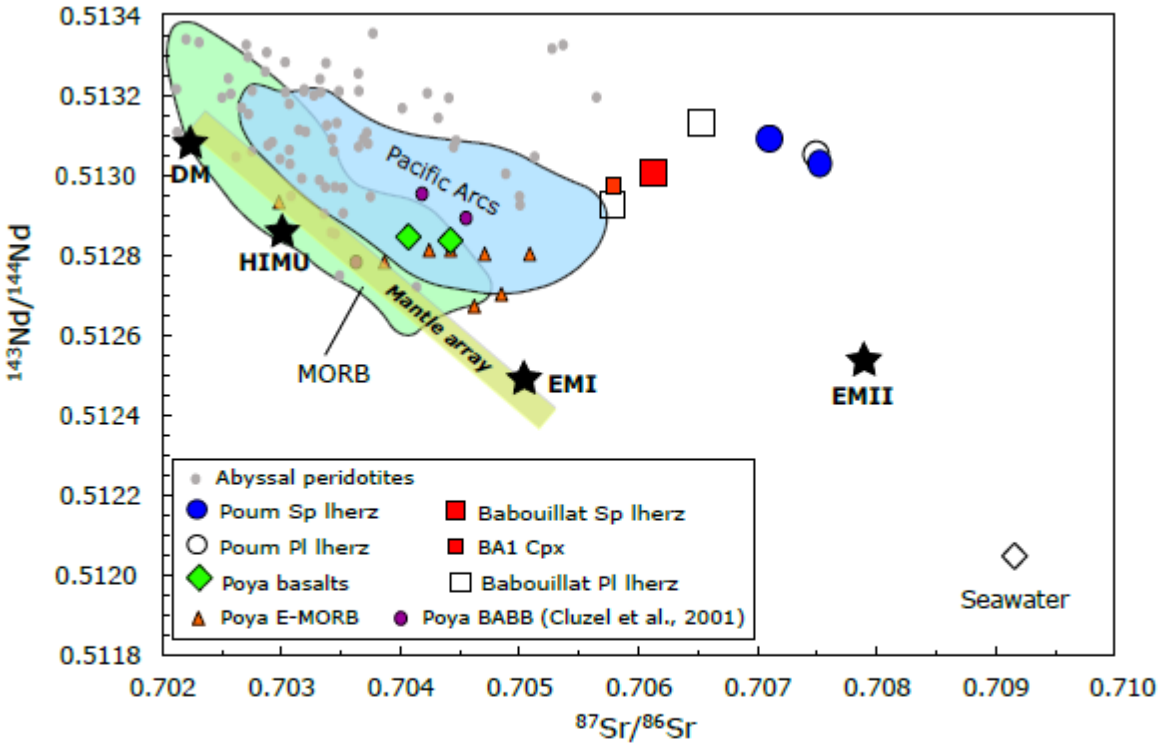

Fig. 6

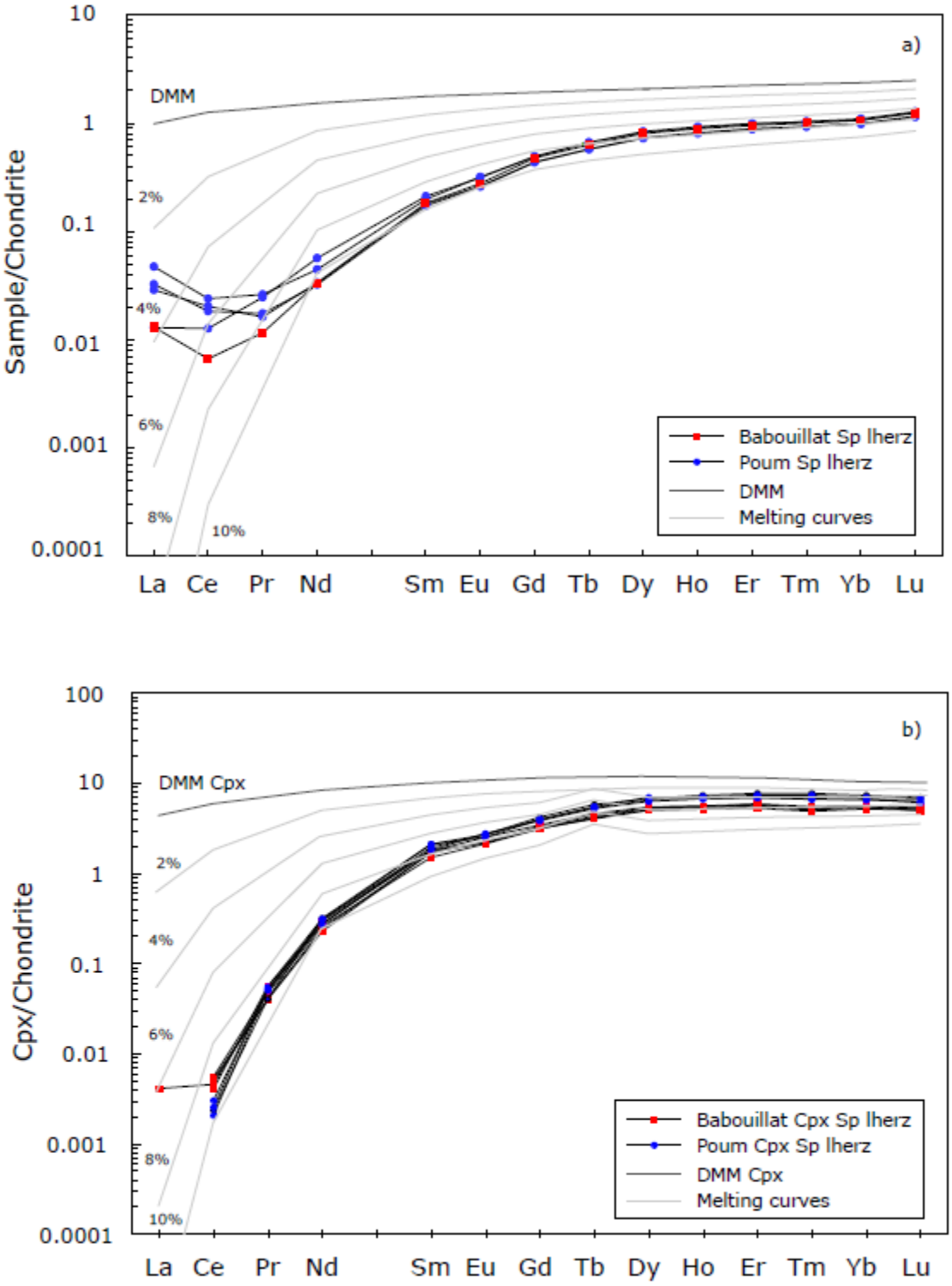

Fig. 7

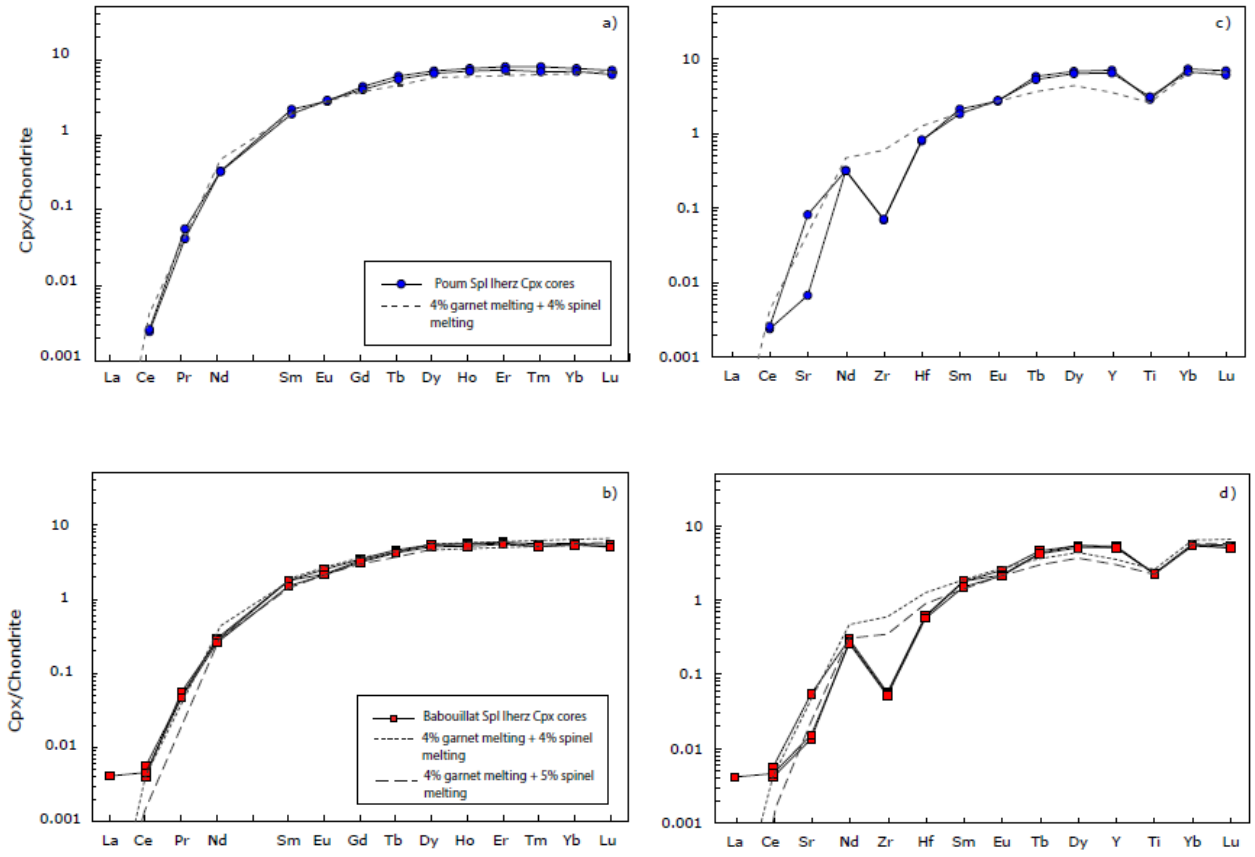

Fig. 8

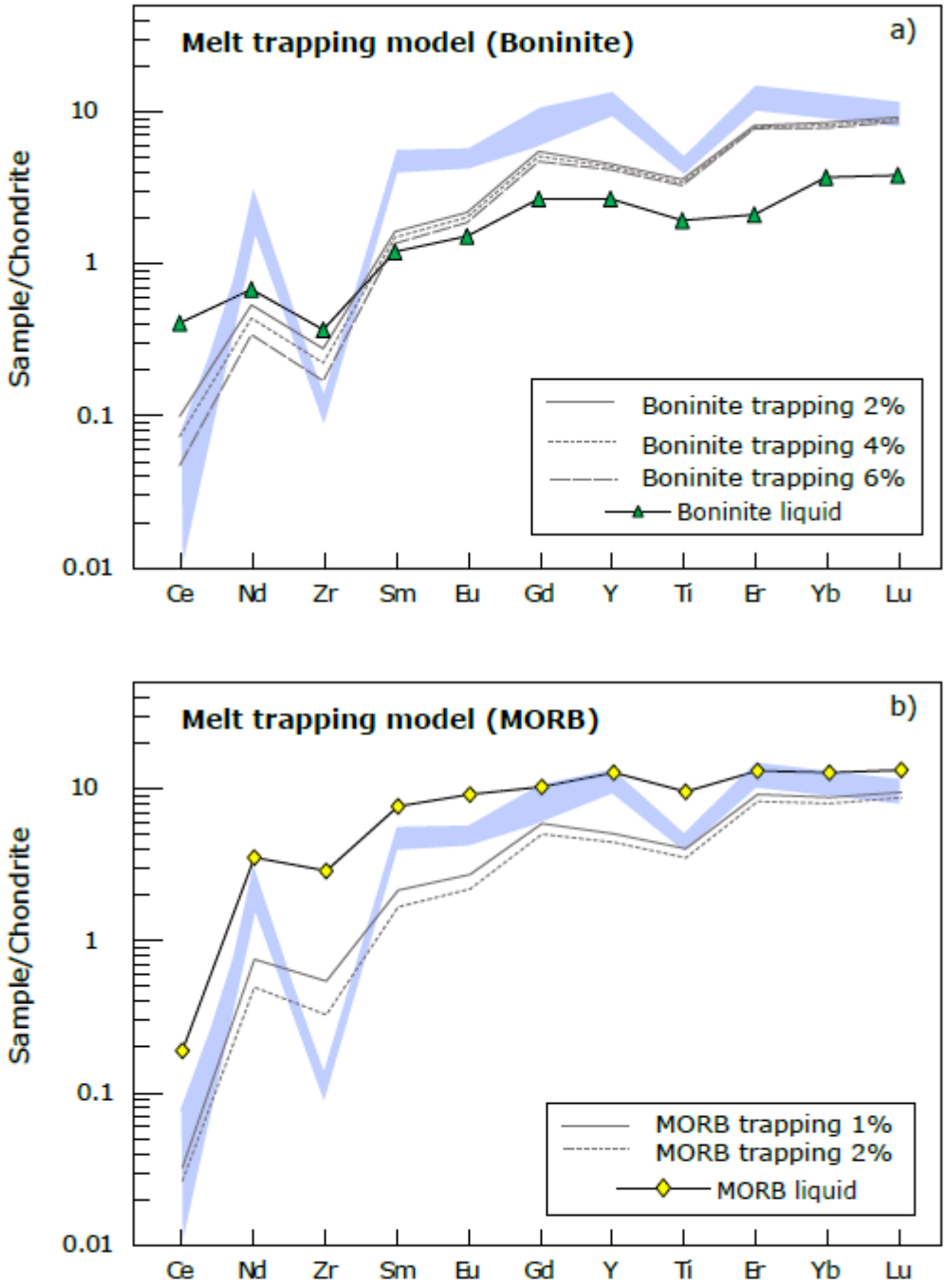

Fig. 9

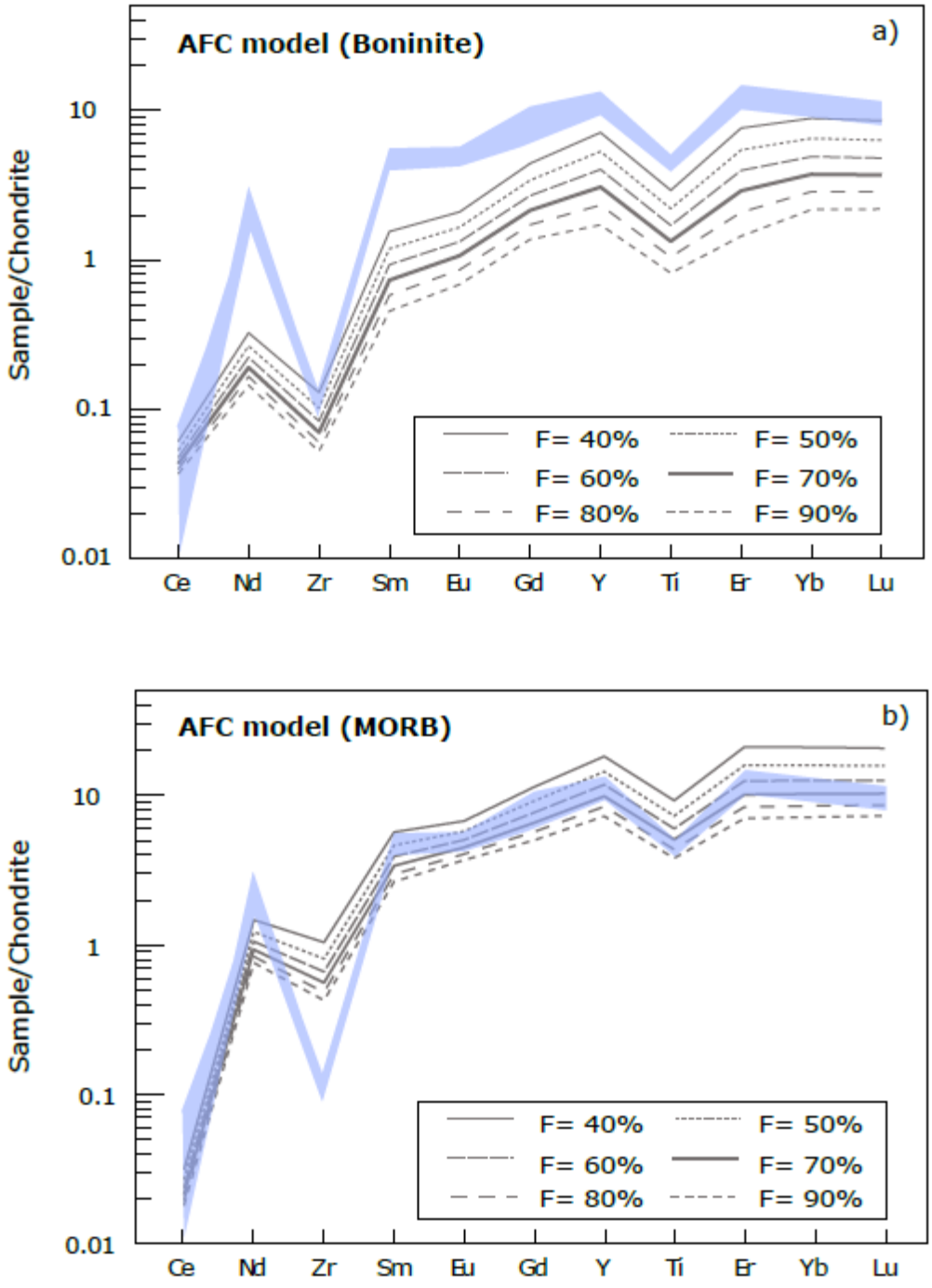

Fig. 10

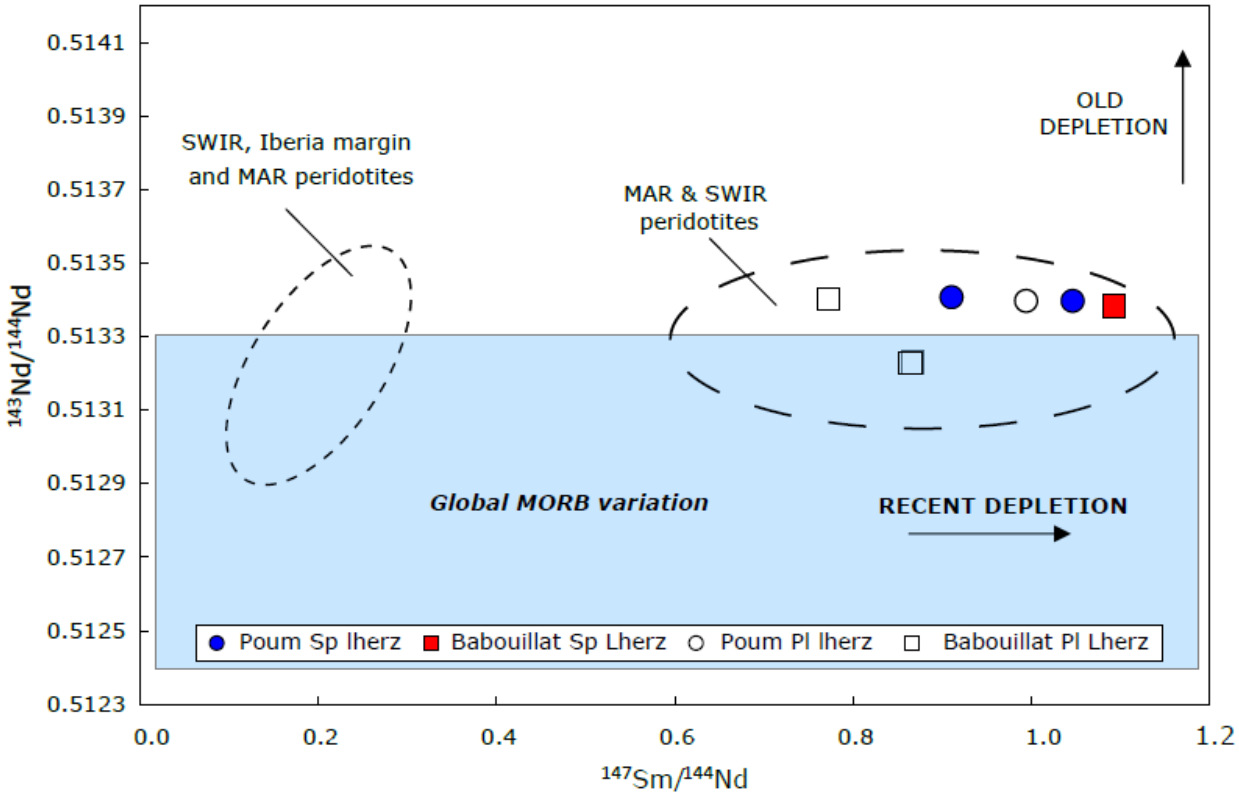

Fig. 11

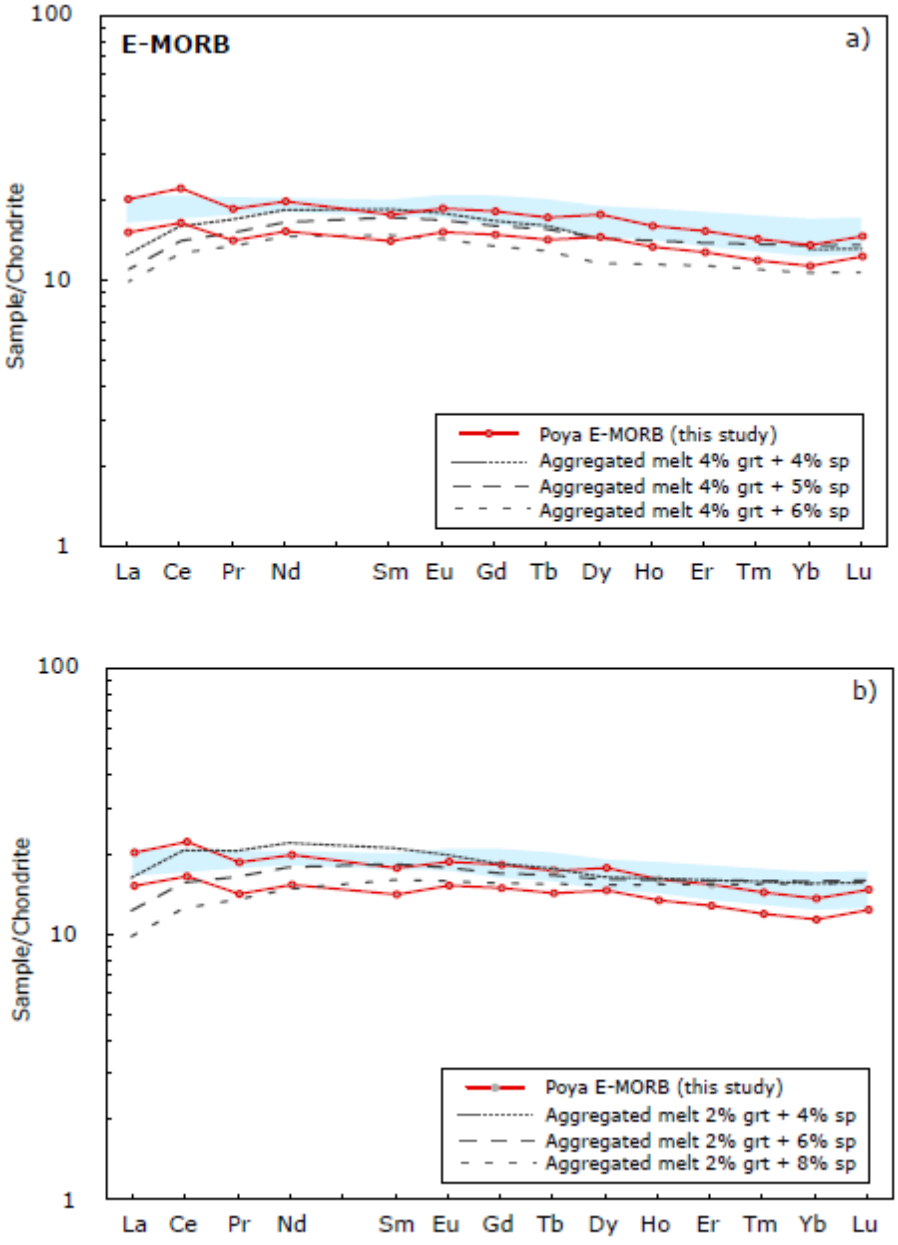

Fig. 12

Table 1: Whole-rock major oxide and trace element data for New Caledonia spinel and plagioclase lherzolites.

Sample	BA1	BA1B	BA2A	BA2B	POU1	POU2	POU3	POU1A	POU2B	BOU1	KO1
Outcrop	Babouillat	Babouillat	Babouillat	Babouillat	Poum	Poum	Poum	Poum	Poum	Bourail	Koné
Rock type	Sp lhz	Pl lhz	Pl lhz	Pl lhz	Sp lhz	Sp lhz	Sp lhz	Pl lhz	Sp lhz	Basalt	Basalt
Latitude	20°22'15.60"S	20°22'43.10"S	20°22'32.20"S	20°22'32.20"S	20°14'09.79"S	20°14'09.79"S	20°14'09.79"S	20°17'41.10"S	20°17'59.30"S	21° 29' 13.5" S	21° 02' 42.5" S
Longitude	164°07'01.70"E	164°07'12.20"E	164°07'07.90"E	164°07'07.90"E	164°00'25.04"E	164°00'25.04"E	164°00'25.04"E	164°02'58.90"E	164°02'13.80"E	165° 24' 49.7" E	164° 52' 26.3" E
Major elements (wt%)											
SiO_2	41.47	41.43	40.56	40.59	40.42	40.12	39.17	40.07	40.78	46.57	47.82
TiO_2	0.04	0.04	0.03	0.04	0.03	0.03	0.03	0.04	0.03	1.13	0.9
Al_2O_3	1.74	2.83	2.80	2.61	1.68	1.46	1.30	2.49	2.57	16.11	15.95
FeO_t	7.32	6.64	7.19	7.31	6.83	6.95	7.00	7.04	6.78	11.42	9.64
MnO	0.12	0.12	0.12	0.12	0.11	0.12	0.11	0.12	0.11	0.21	0.18
MgO	40.21	37.82	39.44	39.51	39.86	40.43	40.75	39.70	36.86	9.06	9.72
CaO	1.91	1.92	1.66	2.03	1.57	1.50	1.26	2.20	1.43	9.12	11.07
Na_2O	0.00	0.04	0.00	0.00	0.00	0.00	0.00	0.00	0.00	2.69	2.06
K_2O	bdl	0.01	0.01	0.01	bdl	bdl	bdl	bdl	bdl	0.06	0.13
P_2O_5	bdl	bdl	bdl	bdl	bdl	bdl	bdl	bdl	bdl	0.08	0.02
LOI	6.39	8.43	7.40	6.98	8.74	8.63	9.60	7.56	10.69	2.41	1.54
Total	99.20	99.28	99.21	99.20	99.24	99.24	99.22	99.22	99.25	98.86	99.03
Mg#	90.74	91.04	90.73	90.61	91.24	91.21	91.22	90.97	90.65		
Trace elements (ppm)											
Cr	2524	2726	2733	2283	2482	2463	2193	2632	2419	186	291
V	70	68	66	64	67	64	57	67	67	349	301
Ni	2042	1945	2040	2037	1974	2034	1995	2025	2008	100	147
Co	124	116	122	124	122	126	126	126	124	53	54
Cu	23	17	23	26	20	24	16	28	0	158	130
Zn	45	43	49	49	43	50	48	51	47	103	91
Rb	0.03	0.16	0.10	0.17	0.03	0.02	0.02	0.09	0.06	0.31	2.59
Sr	0.55	2.19	2.78	3.22	7.19	1.06	3.30	17.80	2.32	122	117
Y	1.21	1.60	1.42	1.45	1.21	1.11	1.04	1.41	1.23	24.05	21.39
Zr	0.06	0.15	0.09	0.10	0.14	0.05	0.05	0.072	0.048	77	51
Nb	0.003	0.004	0.004	0.004	0.003	0.003	0.003	0.003	0.004	5.38	3.73
Cs	0.002	0.077	0.022	0.063	0.001	0.001	0.001	0.003	0.004	0.009	0.202
Ba	0.14	0.49	0.52	0.46	0.14	0.10	0.11	0.89	0.37	51	54
La	0.003	0.004	0.004	0.003	0.003	0.008	0.007	0.004	0.011	4.80	3.59
Ce	0.004	0.007	0.008	0.004	0.008	0.012	0.012	0.006	0.015	13.60	10.07
Pr	0.001	0.003	0.002	0.001	0.002	0.002	0.002	0.001	0.002	1.76	1.34
Nd	0.015	0.040	0.027	0.027	0.026	0.015	0.016	0.023	0.021	9.25	7.14
Sm	0.028	0.051	0.033	0.041	0.032	0.026	0.027	0.036	0.030	2.70	2.15
Eu	0.016	0.028	0.018	0.022	0.018	0.015	0.015	0.021	0.019	1.08	0.88
Gd	0.098	0.149	0.103	0.127	0.102	0.089	0.090	0.118	0.100	3.73	3.05
Tb	0.024	0.034	0.025	0.029	0.025	0.022	0.021	0.027	0.025	0.64	0.53
Dy	0.204	0.280	0.214	0.245	0.209	0.186	0.184	0.233	0.213	4.49	3.70
Ho	0.050	0.066	0.052	0.059	0.051	0.046	0.045	0.056	0.052	0.91	0.76
Er	0.158	0.203	0.163	0.178	0.163	0.146	0.146	0.173	0.164	2.54	2.11
Tm	0.026	0.032	0.026	0.028	0.026	0.024	0.024	0.028	0.026	0.36	0.30
Yb	0.181	0.220	0.182	0.193	0.187	0.168	0.168	0.194	0.181	2.30	1.92
Lu	0.032	0.038	0.033	0.033	0.032	0.030	0.029	0.033	0.032	0.37	0.31
Hf	0.014	0.026	0.019	0.021	0.018	0.014	0.014	0.017	0.013	2.21	1.48
Pb	0.12	0.20	0.18	0.15	0.16	0.17	0.22	0.20	0.14	1.34	2.33

Th	0.001	0.001	0.001	0.001	0.001	0.001	0.001	0.001	0.002	0.44	0.30
U	bdl	bdl	bdl	bdl	bdl	bdl	bdl	bdl	0.004	0.13	0.08

LOI: loss on ignition. Mg# = 100 × cationic Mg/ (Mg+Fe) with all the Fe as Fe2+; bdl = below the detection limit.

Table 2: Sr and Nd isotopic composition for New Caledonia spinel and plagioclase lherzolites.

Sample	BA1	BA1 Cpx	BA1B	BA2B	POU2	POU1A	POU2B	KO1	BOU1
Lithology	*Sp lhz*	*Sp lhz*	*Pl lhz*	*Pl lhz*	*Sp lhz*	*Pl lhz*	*Sp lhz*	Basalt	Basalt
Type	*WR*	*Mineral*	*WR*	*WR*	*WR*	*WR*	*WR*	*WR*	*WR*
Outcrop	Babouillat	Babouillat	Babouillat	Babouillat	Poum	Poum	Poum	Koné	Bourail
Measured ratio									
$^{143}Nd/^{144}Nd$	0.513384 ± 10	0.513407 ± 6	0.513402 ± 8	0.513230 ± 13	0.513398 ± 13	0.513398 ± 8	0.513408 ± 7	0.512915 ± 4	0.512904 ± 5
Sm (ppm)	0.03	0.18	0.05	0.04	0.03	0.04	0.03	2.15	2.70
Nd (ppm)	0.02	0.09	0.04	0.03	0.02	0.02	0.02	7.14	9.25
$^{147}Sm/^{144}Nd$	1.093	1.225	0.772	0.867	1.046	0.994	0.910	0.182	0.176
$^{87}Sr/^{86}Sr$	0.706266 ± 15	0.706024 ± 51	0.706704 ± 5	0.705905 ± 23	0.707572 ± 11	0.707504 ± 12	0.707198 ± 7	0.704114 ± 4	0.704424 ± 5
Rb (ppm)	0.03	0.07	0.18	0.17	0.02	0.09	0.10	2.59	0.31
Sr (ppm)	0.52	0.68	2.21	3.07	1.03	18.84	2.25	117.20	121.61
$^{87}Rb/^{86}Sr$	0.184	0.311	0.230	0.163	0.059	0.014	0.127	0.064	0.007
Age corrected ratio (53 My)									
$^{143}Nd/^{144}Nd_i$	0.513005	0.512982	0.513134	0.512930	0.513035	0.513053	0.513093	0.512853	0.512843
εNd_i	+8.46	+8.01	+10.97	+6.98	+9.05	+9.40	+10.16	+5.48	+5.30
T_{DM} (Ma)	45		75	45	50	53	62		
$^{87}Sr/^{86}Sr_i$	0.706128	0.705791	0.706531	0.705782	0.707527	0.707494	0.707103	0.704066	0.704419
εSr_i	+23.98	+19.19	+29.70	+19.07	+43.85	+43.37	+37.82	-5.29	-0.28

All errors are 2σ and relate to the last significant digits. Decay constants for $^{87}Rb = 1.42 \times 10^{-11} y^{-1}$, for $^{147}Sm = 6.54 \times 10^{-12} y^{-1}$

Highlights

- A new set of geochemical and isotopic (Sr and Nd) data for New Caledonia lherzolites is presented
- The lherzolites underwent a multistage evolution including polybaric fractional melting and plagioclase impregnation
- Nd isotopes indicate a DM mantle source that experienced a recent depletion event
- A possible genetic relationship between the lherzolites and the Poya basalts is evaluated on the basis of geochemical and isotopic data